

## SPECTROGRAPHIC OBSERVATIONS OF PECULIAR STARS. II\*

P. SWINGS AND O. STRUVE

## ABSTRACT

*RX Puppis*.—Besides the strong emission lines of *H*, *He* I, and *He* II, this star is characterized by very intense lines of [*Fe* VII]; other highly ionized elements observed in the spectrum are [*Ne* V], [*Fe* VI], and [*Ca* VII]. The object is very similar to CI Cygni; but the evidence for a late-type component is not as definite. The behavior of the forbidden lines is discussed.

*Recent variations in the spectra of T Coronae Borealis, Z Andromedae, RW Hydrae, RS Ophiuchi, and AX Persei*.—These five objects combine bright lines of high excitation and late-type spectra. In all cases their line-emission spectra observed in the last few years behave in the same way as in novae in their nebular stages; but the ejection velocities are smaller than in single novae, even of the slow type.

*γ Cassiopeiae*.—The observations obtained in 1940 and 1941 were used to determine the contours of the broad lines from the reversing layer. These lines became gradually stronger as the lines produced by the outer shell grew weaker. The optical thickness for continuous radiation of the shell near its maximum development was about  $\tau_{\lambda} = 0.2$ .

*14 Comae Berenices*.—The spectrum of this star consists of (1) an A5 component of moderate luminosity whose *H* lines show strong Stark effect and whose lines of *Mg* II, *Si* II, *Fe* II, and *Fe* I show rapid axial rotation and (2) the spectrum of a shell, which is responsible for sharp *H* $\alpha$  but which is otherwise weak in *H*; the shell also gives rise to sharp lines of *Ti* II, *Cr* II, *Sc* II, *Ca* II, etc., and resembles the spectrum of  $\epsilon$  Aurigae, except that *H* is much weaker and that the excitation temperature is lower. Some spectroscopic peculiarities of the shell may be accounted for by the hypothesis that the pressure within the shell is lower (perhaps by a factor of 10 or 100) than in normal supergiant reversing layers.

COMPLEX OBJECTS OF HIGH EXCITATION<sup>1</sup>I. RX PUPPIS<sup>2</sup>

The variability of this star has been the subject of many discussions. During the thirty-five years prior to 1914 the light-curve showed only one long deep minimum, and for this reason E. C. Pickering<sup>3</sup> suggested that it belongs to the R Coronae Borealis type. This was adopted by H. Ludendorff,<sup>4</sup> who placed RX Pup among the variables belonging "certainly" to the R Coronae class. C. and S. Gaposchkin<sup>5</sup> mention that neither the light-curve nor the spectral observations substantiate the ascription to the R CBr class. The variation is very slow; a period of about twenty years was first suggested,<sup>3</sup> then one of six years.<sup>6</sup> Actually, there was no appreciable change during the interval from 1919 to 1924, and the star now varies slowly and irregularly.<sup>7</sup>

\* *Contributions from the McDonald Observatory, University of Texas*, No. 37. The first paper under this title appeared as *Contribution* No. 22.

<sup>1</sup> References to our papers on complex objects of high excitation and related stars:

Z And: *Pub. A.S.P.*, 51, 297, 1939; *Ap. J.*, 91, 601, 1940; *ibid.*, 93, 356, 1941.

T CBr: *Pub. A.S.P.*, 52, 199, 1940.

R Aqr: *Ap. J.*, 91, 601, 1940.

AX Per: *Ibid.*

CI Cyg: *Ibid.*

RW Hya: *Proc. Nat. Acad. Sci.*, 26, 458, 1940.

IC 4997: *Ap. J.*, 93, 356, 1941.

$\alpha$  Sco: *Ibid.*, 92, 303, 1940.

MWC 17: *Ibid.*, 93, 349, 1941.

CD  $-27^{\circ}11'944$ : *Ibid.*

WY Gem and B 1985: *Ibid.*, 91, 601, 1940; *ibid.*, 93, 455, 1941.

<sup>2</sup> HD 69190; CD  $-41^{\circ}39'11$ ;  $\alpha$  (1900)  $8^{\text{h}}10^{\text{m}}7$ ,  $\delta$  (1900)  $-41^{\circ}24'$ ; max. mag. 11.1; range = 3.0 mag.

<sup>3</sup> *Harvard Circ.*, No. 182, 1914.

<sup>4</sup> *Handb. d. Ap.*, 6, 77, 1928.

<sup>6</sup> *Harvard Bull.*, No. 809, 1924.

<sup>5</sup> *Variable Stars*, p. 319, 1938.

<sup>7</sup> For the light-curve see *Variable Stars*, p. 313, Fig. XI, 1.

The spectrum was first described by Pickering<sup>8</sup> as showing  $H\beta$ ,  $H\gamma$ ,  $H\delta$ , and  $H\zeta$  bright and as being similar to  $\eta$  Carinae. It was described in more detail by Miss A. J. Cannon,<sup>9</sup> who pointed out the resemblance to the spectra of gaseous nebulae or novae and who classified the spectrum as of type Pd, of which the prototype is IC 4997; this assignment was based upon the great strength of the transition of auroral type of  $[O\ III]$ ,  $\lambda\ 4363$ . The bright lines observed by Miss Cannon belong to  $H$ ,  $He\ II$ ,  $[O\ III]$ , and  $[Ne\ III]$ .

C. and S. Gaposchkin have placed RX Pup among the irregular variable stars with spectra showing forbidden lines, and they have emphasized the point that "it is far from certain that AG Pegasi, Z Canis Majoris, and RX Puppis are not, in fact, more nearly novae than anything else." In the nebular variables, RX Pup was placed by C. and S. Gaposchkin among the intrinsic variables, the other typical representative being AG Peg. Recent work by Merrill<sup>10</sup> has now revealed that, contrary to the preceding assumption, AG Peg (BD + 11° 4673) has a red companion and should thus be placed among the double systems, such as Z And or T CBr, rather than among the intrinsic variables. There is some evidence that RX Pup may belong to the same category.

The large drop in brightness which occurred around 1905 may well have been of a nature similar to the deep minimum observed in Nova Herculis; in any case, it is not possible to attribute the object to the R CBr type.

A series of spectrograms of RX Pup was secured in January, 1941, at the McDonald Observatory. The continuous spectrum is confined to the yellow and red region, where it reveals several absorption features. These are identical to the ones observed in MWC 17;<sup>11</sup> but because of the very low dispersion in the red region and the presence of strong emission lines, the suspected red companion cannot be fully ascertained.

*Description of the emission spectrum.*—The measured lines are collected in Table 1. It is evident at once that the star is characterized by very strong lines of  $[Fe\ VII]$ ; for example, the strongest  $[Fe\ VII]$  line at  $\lambda\ 6085$  is as intense as the neighboring line  $D_3$  of  $He\ I$ . RX Pup is, therefore, very similar to CI Cygni and to AX Persei<sup>12</sup> (the latter, as it appeared in 1939; see the following section). Besides  $[Fe\ VII]$ , the other observed lines of high excitation belong to  $[Ne\ V]$ ,  $[Fe\ VI]$ , and  $[Ca\ VII]$ .

Hydrogen, Helium I and II: Many lines are present;  $He\ II\ 4686$  is almost as intense as  $H\beta$ .

Carbon:  $C\ II$  is not observed, but  $C\ III$  is present, and  $C\ IV$  is strong.

Nitrogen: Besides strong permitted  $N\ III$  lines, the spectrum shows  $[N\ II]$  of appreciable intensity.

Oxygen: Very weak permitted  $O\ III$  lines are observed, which are excited by the resonance line of  $He\ II$ . The three forbidden lines of  $[O\ III]$  are very strong. The intensity ratio of the transitions of auroral and nebular type is very similar to that observed in IC 4997,<sup>13</sup> which indicates that the electron density in the nebular regions of  $[O\ III]$  emission is of the order of  $10^5$  to  $10^6$  electrons per cubic centimeter. The intensity ratio of  $\lambda\ 4363$  to  $N_1 + N_2$  is smaller in RX Pup than in the two other high-excitation objects CI Cyg or AX Per (1939), which must have an electron density of the order of  $10^7$  electrons per cubic centimeter.

The nebular transitions of  $[O\ I]$  are also present; they must be excited in outer regions of low electron pressure, as the auroral transition  $\lambda\ 5577$  is not observed. The transition probabilities of  $\lambda\ 6364$  and  $\lambda\ 6300$  are intermediate between those of  $[O\ III]$  and  $[N\ II]$ .

The  $[O\ II]$  lines are absent, and they were also very weak in CI Cyg and AX Per (1939). The fact that  $[N\ II]$  appears, whereas  $[O\ II]$  is absent, despite the similarities in ionization and excitation potentials, is due to the large difference in transition probabilities. The average lifetime of the  $^2D$ -levels of  $O\ II$  is about twenty times as long as the lifetime of

<sup>8</sup> *Harvard Circ.*, No. 17, 1897.

<sup>11</sup> *Ap. J.*, 93, 349, 1941.

<sup>9</sup> *Harvard Ann.*, 76, 19, 1916; *ibid.*, 93, 268, 1919.

<sup>12</sup> *Ap. J.*, 91, 607, 1940.

<sup>10</sup> *Pub. A.S.P.*, 53, 124, 1941.

<sup>13</sup> *Ap. J.*, 93, 356, 1941.

TABLE 1  
EMISSION LINES IN RX PUPPIS

$\lambda$	INT.	IDENTIFICATION		$\lambda$	INT.	IDENTIFICATION	
		Elem.	Lab. $\lambda$			Elem.	Lab. $\lambda$
3426.....	I	[Ne V]	3425.8	4414.3.....	I	[Fe II]	4413.8
3444.....	0	O III	3444.1	4416.4.....	I	[Fe II]	4416.3
3758.9.....	3	[Fe VII] O III	3759.9 3759.9	4471.4.....	2	He I	4471.5
3770.6.....	I-0	H II	3770.6	4490.1.....	in	Fe II [Fe II]	4489.2; 4491.4 4488.8; 4492.6
3798.0.....	I	H <sub>10</sub>	3797.9	4518.2.....	I-on	Fe II	4511.3; 4520.2; 4522.6
3835.3.....	I	H <sub>9</sub>	3835.4	4541.1.....	2	He II	4541.6
3868.1.....	6	[Ne III]	3868.7	4549.7.....	I-0	Fe II	4549.5
3889.1.....	2	H <sub>8</sub> He I	3889.1 3888.6	4555.8.....	I-0	Fe II	4555.9
3967.5.....	3	[Ne III]	3967.5	4570.....	0	(Mg I	4571.1)
3970.1.....	3	H $\epsilon$	3970.1	4583.4.....	I-2	Fe II	4583.8
4027.1.....	0-I	He I	4026.2	4629.2.....	I	Fe II	4629.3
4068.4.....	I	[S II]	4068.5	4634.2.....	2	N III	4634.2
4097.4.....	I-2	N III	4097.3	4640.8.....	3	N III	4640.6
4101.7.....	4-5	H $\delta$	4101.7	4647.0.....	0-I	C III	4647.4
4178.0.....	I-0	Fe II	4178.9	4657.6.....	I-2	C IV [Fe III]	4658.6 4658.2
4199.9.....	I-0	He II	4199.9	4666.8.....	I-0	(C III	4665.9)
4233.1.....	I-0	Fe II	4233.2	4685.9.....	10	He II	4685.8
4243.8.....	I	[Fe II]	4244.0	4713.6.....	I-0	He I	4713.1
4276.3.....	I	[Fe II]	4276.9	4725.0.....	0-I	([Ne IV]	4720.)
4287.2.....	I-2	[Fe II]	4287.4	4729.0.....	0-I	[Fe II]	4728.1
4304.....	0	Fe II	4303.2	4861.3.....	12	H $\beta$	4861.3
4340.7.....	6	H $\gamma$	4340.5	4923.0.....	I	He I Fe II	4921.9 4923.9
4351.5.....	I	Fe II	4351.8	4959.2.....	6	[O III]	4959.5
4358.9.....	I-2	[Fe II]	4359.3	5007.2.....	12	[O III]	5007.6
4363.3.....	5	[O III]	4363.2	5016.8.....	I	He I Fe II	5015.7 5018.4
4386.....	0-I	He I	4387.9				

1941APJ.....94..291S

TABLE 1—Continued

$\lambda$	INT.	IDENTIFICATION		$\lambda$	INT.	IDENTIFICATION	
		Elem.	Lab. $\lambda$			Elem.	Lab. $\lambda$
5158.3.....	2	[Fe VII]	5158.3	5673.8.....	1	[Fe VI]	5678.0
5178.2.....	1	[Fe VI]	5177.0	5720.0.....	4	[Fe VII]	5720.9
5236.0.....	1-2	[Fe VI]	5236.6	5753.0.....	2-3	[N II]	5755.0
5274.5.....	2	[Fe VII] [Fe VI] [Fe III]	5276.1 5279.2 5270.5	5796.3†.....	1	(C IV	5801.5)
5308.7.....	1	[Ca V]	5308.9	5875.0.....	5	He I	5875.6
5316.0.....	1	([Cl IV] Fe II)	5322.2 5316.6	6085.6.....	5	[Fe VII] [Ca V]	6085.5 6085.9
5334.....	1-0	[Fe VI]	5336.4	6306.....	3-4	[O I] [S III]	6300.2 6310.2
5411.4.....	3	He II	5411.6	6365.....	1-2	[O I] [Fe X]	6363.9 6371.
5526.2*.....	1	([Cl III]	5517.2)	6563.....	20	Ha	6562.8
5532.5*.....	1	([Cl III]	5537.7)	6678.....	3	He I	6678.1
5617.0.....	1	[Ca VII]	5619.				

\* Separation uncertain.

† Doubtful line.

<sup>2</sup>D of N II, and the auroral line [N II] 5755 corresponds to an even larger transition probability. Whereas this factor is quite unimportant at very low electron densities, it may become critical for higher densities. On the contrary, the auroral and nebular transitions of [O III] have greater transition probabilities than the corresponding lines of [N II].<sup>14</sup> For the same reason, [S II] is often present in shells of fairly high electron density<sup>15</sup> while [O II] is absent.

Of all the elements likely to appear with appreciable intensity in extended atmospheres, the lines [O II] 3726 and 3729 have the lowest transition probabilities and will be the first to vanish as soon as the electron density reaches a certain critical value. They are, therefore, particularly useful in discussions of electron densities or of stratification effects. Extension of the spectrograms to  $\lambda$  7350 would permit a comparison of the <sup>2</sup>D - <sup>2</sup>P lines at  $\lambda$  7319 and  $\lambda$  7330 (transition probabilities 0.36 and 0.31) with the <sup>4</sup>S - <sup>2</sup>P transitions at  $\lambda\lambda$  3729-3726 (trans. prob. 0.000085 and 0.000068).

Neon: [Ne III] is very strong. Despite the low southern declination ( $-41^\circ$ ) of the star, which caused strong atmospheric absorption in the ultraviolet region, [Ne v] 3426 is observed as a faint line, which indicates that the [Ne v] lines must actually be intense. The forbidden lines of [Ne v] have always been observed when [Fe VII] was present (e.g., in N Her, AX Per, and CI Cyg).

Calcium: As in AX Per and CI Cyg, [Ca v] and [Ca VII] are observed.

Iron: Many lines of Fe II and [Fe II] have been measured, the forbidden lines being, on the average, stronger than the permitted ones. There is no evidence in favor of Fe III,

<sup>14</sup> The numerical values of the transition probabilities may be found in Pasternack's paper, *Ap. J.*, **92**, 129, 1940.

<sup>15</sup> *Ap. J.*, **93**, 455, 1941.

and the presence of [Fe III] is not certain. [Fe V] is absent, whereas [Fe VI] is faintly represented by all its characteristic lines of the  $4F - 2G$  and  $4F - 4P$  forbidden multiplets; actually, RX Pup is richer in [Fe VI] than AX Per (1939) or CI Cyg. [Fe VII] gives many conspicuous lines in the region  $\lambda > 5100$ , where the intensity distribution among the various transitions  $3F - 3P$  and  $3F - 1D$  is very similar to those in Nova Pictoris, CI Cyg, or AX Per (1939). In the ultraviolet,  $3F_4 - 1G_4$  at  $\lambda 3759$  is observed, whereas the weaker transition  $3F_3 - 1G_4$  at  $\lambda 3587$  is not seen on the spectrograms; this is undoubtedly due to the low declination of the object. With our small dispersion in the red region the fairly strong [O I] line at  $\lambda 6364$  precludes the detection of a possible [Fe X] line around  $\lambda 6372$ .

*Conclusions.*—The complex character of RX Pup is not as certain as that of AX Per or CI Cyg, but the far-reaching spectroscopic similarity between these three objects points toward a similar structure. In all three cases we observe strong forbidden lines of [Fe VII], together with fairly strong permitted and forbidden lines of Fe II, whereas the intermediate stages of ionization III and V are absent or extremely weak; in all three objects [Fe VI] is also faint. Obviously, the intensity ratios depend also essentially on the transition probabilities. But at least in two cases, RY Scuti<sup>16</sup> and MWC 17,<sup>17</sup> do we have observational evidence showing that the [Fe III] lines may appear strongly in a shell, together with [N II] and [O III], as in RY Scu, or with [O I], [Fe II], Fe II, [S II], and [N II], as in MWC 17. The fact that the nebular envelopes of several novae (N Pictoris, N Herculis, N Lacertae [1936], and N Serpentis) have shown strong [Fe VII] lines is certainly of significance in connection with the present problem.

## 2. RECENT VARIATIONS IN THE SPECTRA OF FIVE COMPLEX OBJECTS COMBINING BRIGHT LINES OF HIGH EXCITATION AND LATE-TYPE SPECTRA

Our recent investigations of the spectra of peculiar binaries, such as AX Per, CI Cyg, T CBr, RW Hya, Z And, etc., have been concerned especially with the nova-like character of the line emission. In this connection it is important to follow the behavior of these spectra and to discuss their connection with the nova phenomenon. In the cases where the nova-like character of the companion of early type is well established—namely, in T CBr and Z And—the bright lines are fairly sharp; this means that the possible range in ejection velocity is much smaller than is usually found in novae, even of the slow type. Our discussion, together with Kuiper's recent dynamical theory of binaries,<sup>18</sup> leaves little doubt that binary nature may stimulate the process of formation of shells or layers, giving rise to line emission; these layers may very well be stratified and unsymmetrical in structure.

*Nova T Coronae Borealis.*—The appearance of the spectrum in the beginning of 1940, about four years after the last outburst, has been described previously.<sup>19</sup> Spectrograms secured from January to May, 1941, show that the excitation in the emission layers has increased since 1940 and that the intensity of the P Cygni type absorption components of  $H\beta$  and  $H\alpha$  has decreased as compared to the bright components. An appreciable increase in intensity is apparent for bright He II 4686 (compared to  $H\beta$ ), for the He I lines (compared to  $H$ ), and for the O III and N III fluorescence lines. The increase in intensity—which evidently runs parallel to that of He II—is apparent even in the short interval between January and May, 1941. The difference in radial velocity of  $H$  and He I, which was reported in 1940, has been maintained, so that the lines  $H_8$  3889.05 and He I 3888.65 are still well separated ( $\Delta\lambda_{\text{obs}} \gg 0.4 \text{ \AA}$ ). But the change in relative intensity of the two lines is very striking.

<sup>16</sup> *Ap. J.*, **91**, 581, 1940.

<sup>17</sup> *Ap. J.*, **93**, 349, 1941. See also the description of the spectrum of DO Aqu 1925, by Vorontsov-Velyaminov, *Ap. J.*, **92**, 283, 1940.

<sup>18</sup> *Ap. J.*, **93**, 133, 1941.

<sup>19</sup> *Pub. A.S.P.*, **52**, 199, 1940.

Gradually, T CBr increases in excitation, exactly as is the case in the beginning of the nebular stages of novae. Compared to the early-type component, the red companion is much more luminous than in AX Per, CI Cyg, and Z And. The spectrum is approaching a stage similar to that of RW Hydrae,<sup>20</sup> and it will be interesting to see whether it will come to a standstill at about that same stage of moderate excitation or whether it will progress toward a still higher excitation, such as in CI Cyg. At present, the evolution is strikingly similar to that of Z And.

*Z Andromedae.*<sup>21</sup>—During the interval from August, 1940, to January, 1941, the most striking spectral variations were:

- a) The increase of the intensity ratio of the nebular to the auroral transitions of [O III];
- b) The disappearance of the P Cygni absorption features and the appearance of a Balmer continuum in emission (instead of absorption).

This is, of course, what would be expected in a post-nova. The same behavior of the [O III] lines appears when we compare our spectrograms of Nova Herculis taken in April, 1940, and in May, 1941; there is a striking change in the decrease of [O III] 4363 compared to  $N_1$  and  $N_2$ , and this must be due to the decrease in the electron density in the expanding ejected nebulosity.<sup>22</sup>

*RW Hydrae.*—Since the time of our description of this spectrum,<sup>23</sup> based upon spectrograms of April, 1940, the early-type companion has been slowly gaining in excitation. On spectrograms of May, 1941, it is apparent that the intensity ratios  $He\ II/He\ I$  and [O III] 4363/ $He\ I\ 4388$  have increased. A remarkable feature of this spectrum, observed in both seasons, is the relatively great intensity of the  $2^1P^0 - n^1D$  lines of  $He\ I$ , as compared to the lines of  $2^3P^0 - n^3D$ . In this respect RW Hya bears a certain resemblance to Z And. On the other hand, in planetary nebulae and in stars of high excitation, such as AX Per, CI Cyg, and RX Pup, the singlet lines are very much weaker than the triplets. The ordinary laboratory spectrum of  $He\ I$  also shows the triplet lines to be much stronger than the singlets, but in certain laboratory experiments abnormally strong singlet lines have been observed. It is not clear why the stars of relatively low excitation—RW Hya, Z And, and perhaps also RS Oph—should show abnormally strong singlet lines. On general grounds we should expect that for very low pressures the singlets will be favored as long as the excitation energies are low and the recombination processes are relatively unimportant. However, the strength of  $He\ II\ 4686$  suggests that recombination must play an important role in  $He\ I$ , unless the gas is stratified.

The excitation in the nebular component is much lower than in CI Cygni and is rather similar to that of T CBr or Z And.

*Nova RS Ophiuchi 1898, 1933.*—This is a recurrent nova, which was included by Merrill and Burwell<sup>24</sup> in their table of objects with dark  $TiO$  bands and bright  $He\ II\ 4686$ . During the sudden outburst of 1898 the spectrum was photographed at the Harvard Observatory;<sup>25</sup> the hydrogen lines from  $H\beta$  to  $H\zeta$  were bright, as were also  $\lambda\ 4640$  and  $\lambda\ 4686$ ; there was a trace of  $He\ I\ 4472$ . From the light-variations<sup>26</sup> the star was considered to be somewhat similar to P Cygni, T Coronae, and  $\eta$  Carinae. A spectrogram was taken in 1923 by Adams, Humason, and Joy,<sup>27</sup> twenty-five years after the first observed out-

<sup>20</sup> *Proc. Nat. Acad. Sci.*, **26**, 458, 1940.

<sup>21</sup> *Ap. J.*, **93**, 356, 1941.

<sup>22</sup>  $He\ II\ 4686$  and  $N\ III\ 4634-4640$  have also increased in intensity compared to  $N_1$  and  $N_2$ , which tends to reduce the green color of the nebulosity of N Her.

<sup>23</sup> *Proc. Nat. Acad. Sci.*, **26**, 458, 1940.

<sup>24</sup> *Ap. J.*, **78**, 87, 1933.

<sup>25</sup> *Harvard Ann.*, **96**, 1921 (HD 143454); **55**, 47, 1907; **76**, 37, 1914.

<sup>26</sup> *Harvard Ann.*, **55**, 7, 1907; *Harvard Circ.*, No. 99, 1905.

<sup>27</sup> *Pub. S.A.P.*, **39**, 365, 1927.

burst; the star was then of magnitude 11.5. It showed strong bright  $H\beta$  and fainter emission at  $H\gamma$ ;  $Fe\ II$  was present as faint emission; there was no certain evidence of bright bands at  $\lambda\ 4640$  and  $\lambda\ 4686$ . An absorption spectrum was observed, but it was difficult of classification, appearing to be about of type G5. During the period 1900–1933, “apart from its rather small range and its persistent variability at minimum (in which it is indeed paralleled by several other novae) there was nothing to set it apart from other novae. . . . In light curve and in spectrum, it is, in the main quite typical.”<sup>28</sup>

The outburst of 1933 was observed spectroscopically at the Mount Wilson and Lick observatories; the star reached a magnitude of 4.3. The spectral changes were very similar to those seen in normal novae; but, according to Adams and Joy,<sup>29</sup> “the great displacements of the absorption lines toward the violet in the earlier stages of the spectra of novae have not been observed.” This point is important, as it shows a great similarity to Z And and T CBr in both of which the ejection velocities were also relatively small. In Z And the radial velocities were  $-68$  km/sec for the absorption lines and  $+30$  km/sec for the emissions;<sup>30</sup> according to measures by Wright and Neubauer,<sup>31</sup> the absorption lines of RS Oph were displaced about  $5\text{\AA}$  with respect to the emissions, suggesting a velocity of ejection three or four times larger than in Z And. Adams and Joy<sup>32</sup> noticed that  $\lambda\ 4363$  was much stronger, relative to  $N_1$  and  $N_2$ , than in normal planetaries. Soon after the outburst, when bright lines of  $H$ ,  $He\ I$ , and  $He\ II$  were also present, Adams and Joy<sup>33</sup> discovered in the spectrum five coronal lines, the intensity of the green line  $\lambda\ 5303$  being comparable to  $H\beta$ . This is the only instance in which the coronal lines have been observed in a nova.

In 1934, when the star had faded to magnitude 11, Adams and Joy<sup>34</sup> found that the spectrum had approximately reverted to that observed in 1923, ten years before the second outburst, the only marked difference being the greater intensity of  $\lambda\ 4686$  in 1934. The coronal lines had disappeared, and the relative intensity of the continuous spectrum had greatly increased.

Humason took a new spectrogram in 1936, three years after the last outburst;<sup>35</sup> the star was approximately of visual magnitude 11.8. He also re-examined the previous spectrogram of 1923 and questioned the type G5 which had been tentatively suggested for the continuous spectrum. His spectrogram of 1936 shows in emission  $N_1$ ,  $N_2$ ,  $H\beta$ ,  $H\gamma$ , and  $H\delta$ . “The continuous spectrum is much stronger, relative to the emission lines, than on the 1923 plate and extends well into the violet. No absorption lines can be seen.” Quite recently Merrill<sup>36</sup> expressed the opinion that RS Oph may possibly belong to the group of stars with bright  $\lambda\ 4686$  and dark  $TiO$  bands.

Two spectrograms secured at the McDonald Observatory in May, 1941, reveal a very strong continuous spectrum whose intensity distribution in the visual region is very similar to that of the continuous spectrum of the similar star RW Hya; on the other hand, just as in Z And and T CBr, the continuous spectrum extends into the blue region. There is no doubt that we have here another case of a composite spectrum, one component being of late spectral type (around K8 or M0), while the other component gives a weak, but definitely blue, continuum. Because of the red companion, only strong emission lines can be seen in the visual region. The measured lines are as follows:

#### BRIGHT LINES PRESENT IN 1941 IN NOVA RS OPHIUCHI

$H$ :  $H\alpha$  (15),  $H\beta$  (8),  $H\gamma$  (5),  $H\delta$  (3),  $H\epsilon$  (1) (blended with [ $Ne\ III$ ]),  $H_8$  (1–0)  
 $He\ I$ : 5876 (8); 5016 (2), 4922 (2), 4713 (1), 4471 (1), 4388 (1), 4121 (1–0)

<sup>28</sup> C. and S. Gaposchkin, *op. cit.*, p. 260.

<sup>29</sup> *Pub. A.S.P.*, 45, 249, 1933.

<sup>30</sup> *Pub. A.S.P.*, 51, 297, 1939.

<sup>31</sup> *Pub. A.S.P.*, 45, 251, 1933.

<sup>32</sup> *Ibid.*, p. 249.

<sup>33</sup> *Ibid.*, p. 301.

<sup>34</sup> *Pub. A.S.P.*, 46, 223, 1934.

<sup>35</sup> *Ap. J.*, 88, 228, 1938.

<sup>36</sup> *Spectra of Long-Period Variable Stars*, p. 105, 1940.

TABLE 2  
EMISSION LINES IN AX PERSEI (JANUARY 15, 1941)

$\lambda$	INT.	IDENTIFICATION		$\lambda$	INT.	IDENTIFICATION	
		Elem.	Lab. $\lambda$			Elem.	Lab. $\lambda$
3868.7.....	4	[Ne III]	3868.7	4520.9.....	1-on	(Fe II	4522.6)
3889.0.....	2	H <sub>8</sub> He I	3889.0 3888.6	4541.7.....	2n	He II	4541.6
3961.6.....	1	O III	3961.6	4555.3.....	0-1	Fe II	4555.9
3964.7.....	1-2	He I	3964.7	4571.8†.....	0	(Mg I	4571.1)
3967.7.....	2	[Ne III]	3967.5	4583.6.....	1-0	Fe II	4583.8
3969.9.....	3	H $\epsilon$	3970.1	4629.0.....	1	Fe II	4629.3
4009.3.....	1	He I	4009.3	4634.2.....	2-3	N III	4634.2
4026.1.....	2	He I	4026.2	4640.6.....	4-5	N III	4640.6
4069.2*.....	1-2	C III [S II]	4069.0 4068.5	4646.3.....	3	C III	4647.4
4071.8*.....	2	C III ([Fe V]	4070.4 4071.5)	4649.5.....	3n	C III C III O II	4650.2 4651.3 4649.1
4075.3.....	1-0	[S II]	4076.5	4659.1.....	0-1	C IV ([Fe III	4658.6 4658.2])
4097.3.....	4	N III	4097.3	4665.9.....	0-1	C III	4665.9
4101.2.....	3	H $\delta$	4101.7	4685.5.....	10	He II	4685.8
4103.0.....	4	N III	4103.4	4713.5.....	2	He I	4713.1
4120.9.....	1	He I	4120.8	4861.6.....	10	H $\beta$ He II	4861.3 4859.4
4144.5.....	2-3	He I	4143.8	4921.6.....	2-3	He I	4921.9
4169.4.....	0	He I	4169.0	4959.5.....	2	[O III]	4959.5
4196.5.....	0-1	N III	4195.7	5007.5.....	4	[O III]	5007.6
4200.6.....	1n	N III He II	4200.0 4199.9	5015.2.....	1	He I	5015.7
4233.4.....	1	Fe II	4233.2	5041.0†.....	1-0	.....	.....
4245.5.....	0-1	[Fe II]	4244.0	5048.7.....	1-0	He I	5047.7
4266.7.....	1	C II	4267.2	5412.0.....	2	He II	5411.6
4288.2.....	0	[Fe II]	4287.4	5721.....	0	[Fe VII]	5720.9
4339.0.....	2	He II	4338.7	5875.6.....	7	He I	5875.6
4340.8.....	7	H $\gamma$	4340.5	6085.....	0	[Fe VII]	6085.5
4363.5.....	5	[O III]	4363.2	6563.....	15	H $\alpha$ He II	6562.8 6560.2
4388.0.....	2-3	He I	4387.9	6678.....	2	He I	6678.1
4471.8.....	3	He I	4471.5				

\* Separation difficult.

† Observed in many high-excitation objects; probably unidentified.

‡ Also present in NGC 7027, NGC 6572, and RY Scuti.



<i>He</i> II:	4686 (6)
[ <i>O</i> II]:	Absent
[ <i>O</i> III]:	4363 (2), <i>N</i> <sub>1</sub> (1), <i>N</i> <sub>2</sub> (1-0)
<i>O</i> III:	3444 (0), 3760 (0)
<i>N</i> III:	4097 (2), 4634-4640 (2)
[ <i>Ne</i> III]:	3869 (2), 3967 (1, blend with <i>He</i> )
[ <i>Ne</i> V]:	Absent
[ <i>S</i> II]:	4068 (0-1)
<i>Fe</i> II:	4233 (0-1), 4352 (1-0), 4576 (1-0), 4584 (1-0)
[ <i>Fe</i> II]:	4244 (0-1), 4359 (0-1)

At present all the lines are rather sharp, and the whole appearance of the spectrum is quite similar to that of other binaries consisting of an M (or late K) component and of a nebulosity of moderate excitation, such as RW Hya or T CBr. As far as the essential

TABLE 3  
TRANSITION PROBABILITIES AND  
EXCITATION POTENTIALS

Element	$\lambda$	Excitation Potential (in Volts)	Transition Probability*
[ <i>O</i> III].....	4363.2	5.3	2.8
	5007.6	2.5	0.016
	4959.5	2.5	0.0056
[ <i>Ne</i> III].....	3967.5	3.2	0.065
	3868.7	3.2	0.21
[ <i>Ne</i> V].....	3425.8	3.8	0.31
[ <i>Fe</i> VII].....	6085.5	2.2	0.49
	5720.9	2.2	0.30

\* According to S. Pasternack, *Ap. J.*, 92, 129, 1940.

physical processes are concerned, the evolution of RS Oph after the 1933 outburst has been similar to that of T CBr or Z And; the main difference between Z And and RS Oph is that the former has a higher excitation and a lower velocity of ejection.

*AX Persei*.—Spectrograms taken in January and May, 1941, show a large change since 1939 and the beginning of 1940,<sup>37</sup> and the object had resumed a state very similar to that of 1931-1932, when Merrill examined it spectroscopically.<sup>38</sup> The principal changes between February, 1940, and January, 1941, are:

- The almost complete disappearance of the lines of [*Fe* VII] and [*Fe* VI], which were conspicuous in 1939, especially [*Fe* VII] in the visual region;
- The considerable increase in intensity of *N*<sub>1</sub> and *N*<sub>2</sub> compared to  $\lambda$  4363;
- A large increase in the intensity ratio of [*Ne* III] and *H*; in 1939,  $\lambda$  3888 was much stronger than [*Ne* III], whereas the opposite is true in 1941.

The variations between February, 1940, and January, 1941, will be discussed first. The list of lines observed in the region  $\lambda\lambda$  3850-6700 on January 15, 1941, is given in Table 2. Table 3 lists some of the transition probabilities and excitation potentials needed in the discussion.

It is necessary to be careful in considering excitation criteria in an object, such as AX Per, in which effects of stratification and asymmetry may be important; for exam-

<sup>37</sup> *Ap. J.*, 91, 607, 1940.

<sup>38</sup> *Ap. J.*, 77, 44, 1933.

ple, the emission of the forbidden  $[Fe\ VII]$  transitions and of the permitted  $H$  or  $He\ I$  lines may be localized in different regions. If we assume that  $[Fe\ VII]$  is localized in a different region than  $[O\ III]$  or  $[Ne\ III]$ , we may think of some occultation effect; but this seems rather unlikely.

If we assume that  $[Fe\ VII]$  was emitted in a region similar to that of  $[O\ III]$  or  $[Ne\ III]$ , except possibly for greater proximity to the exciting center, it is certain that the electron temperature in the emitting regions has not changed greatly. The presence of  $N_1$ ,  $N_2$ ,  $\lambda\ 4363$ , and  $[Ne\ III]$  shows that the electron temperature would have been high enough to excite  $Fe\ VII$  ions on their metastable levels. The electron density has decreased, as is shown by the decrease in the intensity ratio  $\lambda\ 4363/N_1, N_2$ . This ratio is now very similar to that of  $Z\ And$  in 1940,<sup>39</sup> but it is still greater than in IC 4997. The electron density must therefore be around  $10^6$  electrons per cubic centimeter in the  $[O\ III]$  region.<sup>40</sup> In 1939 the intensity ratio of  $\lambda\ 4363$  to  $N_1$  must have required a much higher density—say of the order of  $10^7$  electrons per cubic centimeter. Let us assume that the electron density has been reduced by a factor of the order of 10 in all emitting layers. Such a reduction could not by itself weaken the  $[Fe\ VII]$  transitions very greatly, as compared to the other ions. From Table 3 it is seen that the transition probabilities of the strongest  $[Fe\ VII]$  lines are intermediate between those of  $\lambda\ 4363$  and of  $[Ne\ III]$ . In 1939 both  $\lambda\ 4363$  and  $[Ne\ III]$  were weaker than  $[Fe\ VII]$ , whereas they are still present in 1941, despite the disappearance of  $[Fe\ VII]$ . Besides, the presence of strong  $N_1$  and  $N_2$ , together with weaker  $\lambda\ 4363$  and  $[Ne\ III]$  in RX Puppis (see preceding section), does not prevent  $[Fe\ VII]$  from attaining a considerable intensity in this star.

We are probably concerned with a change in the ionization of the region where  $[Fe\ VII]$  is emitted. In an expanding nebulosity exposed to a constant exciting nucleus, the change in ionization depends essentially on the ratio of the dilution factor and of the electron density. It is difficult to make any numerical calculations in the present case; but it does not seem reasonable to suppose that the expansion would give rise to almost complete disappearance of  $[Fe\ VII]$ , while the rest of the spectrum is not fundamentally altered.

There is, thus, no escape from the conclusion that the exciting nucleus must have changed appreciably during the last year. Such a change will influence the ionization of distant layers only after a certain lag, which evidently varies with the distance to the nucleus and with the density.  $[Fe\ VII]$  was probably excited in the region closest to the nucleus and should be first to react to a nuclear variation. It is well known that a post-nova nucleus fluctuates in brightness; and in case of a surrounding nebulosity this will obviously give rise to a variation of the excited nebular spectrum after certain relaxation times  $\Delta t$ , which are functions of the nebular density and of the distance from the nucleus.

In the case of Nova Pictoris, which is the best representative of a nova with strong  $[Fe\ VII]$  lines, these lines attained a maximum of intensity around 1932, compared to  $He\ II\ 4686$  and  $H\alpha$ , and then decreased during the following years. Actually, except for the width of the lines, the spectrum of AX Per in 1939 was very similar to that of N Pic in September, 1926.<sup>41</sup> In N Pic,  $[Fe\ VII]\ 6085$  was stronger than  $He\ II\ 4686$  in 1931–1932, whereas the opposite was true in 1933; in 1934,  $\lambda\ 4686$  was the strongest line of the spectrum,  $H\alpha$  came next, with  $\lambda\ 6085$  nearly as strong. As the behavior of the intensity ratio of  $\lambda\ 4363$  and  $N_1$  in AX Per is of the type observed in novae, the comparison to N Pic is justified.

When Merrill observed AX Per in 1931–1932, the intensity ratio of  $\lambda\ 4363$  and  $N_1, N_2$  was similar to that which we observed in January, 1941; no appreciable variation was

<sup>39</sup> *Ap. J.*, **93**, 356, 1941.

<sup>40</sup> Yet the possibility still exists that  $\lambda\ 4363$  and  $N_1-N_2$  are not emitted in the same region.

<sup>41</sup> Spencer Jones, *M.N.*, **94**, 35, Pl. I, 1933.

observed by Merrill over a period of one year. It is tempting to think of some recurrent phenomenon. The presence of a variable red companion makes any connection with the light-curve rather problematic.

During the period from January 15 to May 30, 1941, new changes have taken place. In May,  $[Ne\ III] 3868.7$  has again become much weaker than  $H_8 3888$ . In January,  $N\ III 4640$  was appreciably stronger than  $He\ I 4472$ , whereas the opposite is true now.  $N_1$  and  $N_2$  have decreased in intensity. Our spectrogram of May 30 extends to  $\lambda 3400$  and shows that the following lines are present:  $[Ne\ V] 3426 (2)$ ,  $O\ III 3444(0-1)$ , and  $O\ III 3759 (2)$ ; the two  $O\ III$  lines belong to the incomplete multiplets excited by  $He\ II$ .  $[O\ II]$  is absent. There is no definite evidence for  $[Fe\ VII]$ .<sup>41a</sup>

*Conclusions.*—In all the five cases considered here the line-emission spectrum behaves in the same way as in novae in their nebular stages. On the whole, the density decreases in the shell, and the excitation increases; but the fluctuations of the novae also produce nebular variations, and in some cases the phenomena are recurrent. The similarity of the five peculiar binaries to novae is well established, but the ejection processes are in all five cases slower than in single novae.

The continued study of peculiar stellar spectra has brought out what looks like a very significant fact: whenever an otherwise normal stellar spectrum of advanced type, which is not expected to show emission lines, is complicated by forbidden and permitted emissions of excitations far beyond those normally associated with the types of these stars, we either find more or less conclusive evidence of the binary nature of these stars or, in a few cases, we find at least no obstacles to the assumption that a faint, hot companion to a late-type star excites the emission lines in a gas of very low density, which (in the case of  $\alpha\ Sco$ ) is distributed in the form of a small nebulosity around the system but which in other cases may well be concentrated in the outermost layers of the late-type component.

The outbursts of Z And, RS Oph, and T CBr show that binaries of the type considered are subject to recurrent nova outbursts on a relatively small scale. But even though the similarity of the spectroscopic history of these binaries with typical large-scale novae is very striking, there is, as yet, no evidence that the physical causes of the outbursts are similar.

#### $\gamma$ CASSIOPEIAE

A brief account of the recent spectrographic history of  $\gamma$  Cassiopeiae has been given by Wellmann.<sup>42</sup> When our series of observations was started at the McDonald Observatory in January, 1940, the entire spectrum was dominated by sharp absorption lines of  $H$ ,  $He\ I$ , and  $Fe\ III$  (Pl. VIII). There was a marked effect of dilution which showed itself in the enhancement of those lines of  $He\ I$  and  $Fe\ III$  which have their origin in metastable levels. The lines of  $H$ ,  $He\ I$ ,  $O\ II$ ,  $O\ III$ ,  $Si\ III$ ,  $Si\ IV$ ,  $C\ II$ ,  $C\ III$ ,  $N\ II$ , and  $Mg\ II$  show, besides, the normal, rotationally broadened lines of a Bo star. Since the shell is strong in  $Fe\ III$  and  $He\ I$  but shows no  $He\ II$ , it probably corresponds to a state of ionization which is similar to, or slightly lower than, that of the reversing layer.

During the past year the sharp absorption lines have gradually become weaker, and since about the first of the year all vestiges of the absorptions at  $He\ I 3889$  have disappeared. From the beginning of January until the end of the series, some time in April, 1941, the spectrum has resembled a normal, broad-lined absorption B star, with fairly

<sup>41a</sup> Added in proof: Spectrograms of AX Per secured on August 2 and 8, 1941, show that  $[Fe\ VII]$  and  $[Ne\ V]$  have recovered their intensities and are now similar to those observed in 1939.

<sup>42</sup> *Beobachtungs-Zirkular d. A.N.*, 23, No. 3, 13, 1941; see also Struve and Elvey, *Pub. A.S.P.*, 52, 140, 1941; Swings and Struve, *Ap. J.*, 91, 589, 1941; Baldwin, *Ap. J.*, 93, 333, 1941; Struve and Swings, *Harvard Announcement Card*, No. 545, 1940; Struve and Greenstein, *Harvard Announcement Card*, No. 551, 1940.

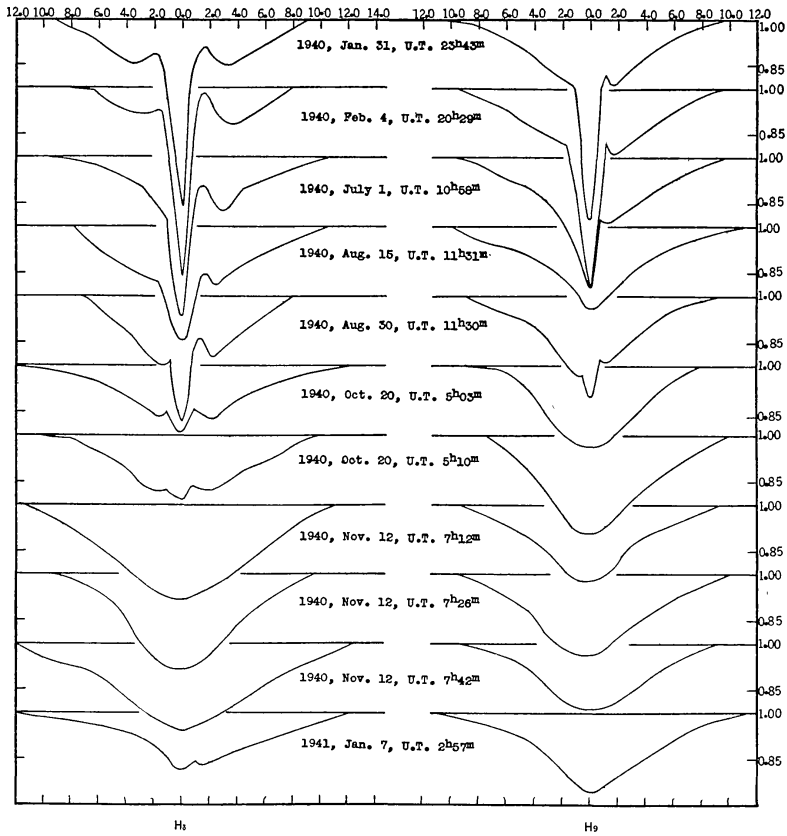


FIG. 1.—Contours of  $H\delta$  and  $H\gamma$  in  $\gamma$  Cassiopeiae. The abscissae are angstrom units; the ordinates are intensities in units of the intensity of the continuous spectrum. In each contour the violet is plotted on the right side of the center.

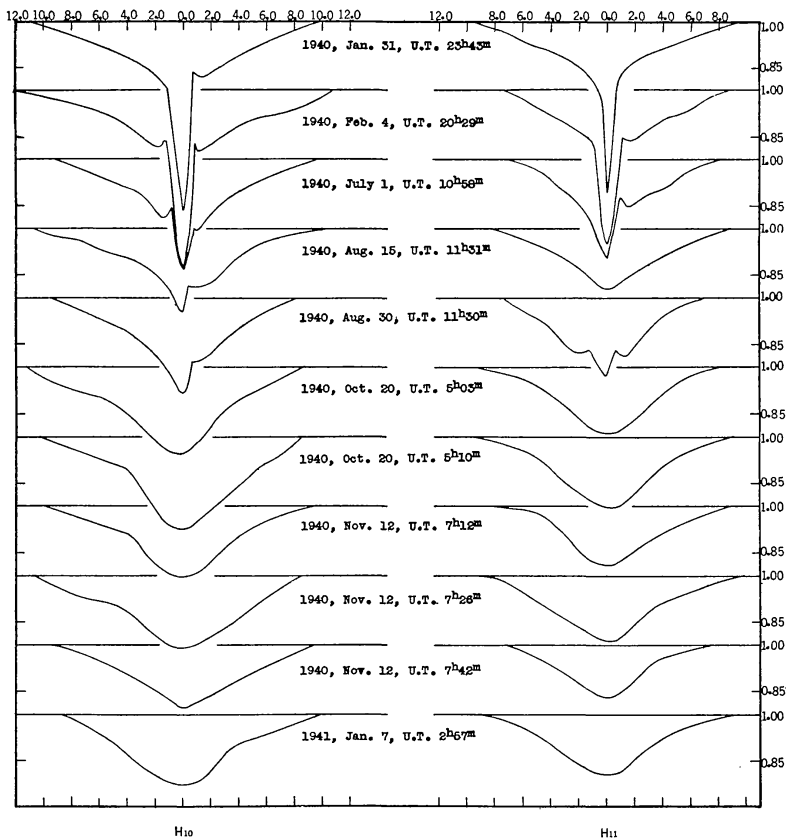


FIG. 2.—Contours of  $H_{10}$  and  $H_{11}$  in  $\gamma$  Cassiopeiae. Violet is on the right side

strong  $H\alpha$  emission but with only a faint suspicion of a central emission in the higher members of the Balmer series.

During the course of the observations visual inspection of the plates led us to suspect that the fading of the sharp absorption lines was accompanied by a marked increase in the intensities of the underlying, rotationally broadened lines from the reversing layer. Since this phenomenon promises to throw some light upon the question of continuous absorption in the shell,<sup>43</sup> we give in Figures 1, 2, and 3 the contours of several lines measured on our best plates. The accidental errors of such measurements are large, and the variations from plate to plate are perhaps not always real. In Figure 4 we show a comparison of the mean contour derived from the first two contours of the series (when the lines of the shell were strong) and from the last four contours (when the lines of the shell were very weak or absent). These mean curves bring out the following results:

1. Those of the underlying lines which are not complicated by emission or absorption in the shell—namely, the blend of several lines of  $O\ II$  at  $\lambda\ 4070$  and the blend of  $Si\ IV$  and  $O\ II$  at  $\lambda\ 4089$ —show a marked strengthening in intensity and equivalent breadth; approximately we can say that a point on the contour without shell absorption, corresponding to an intensity of 90 per cent of the continuous spectrum, has an intensity of 93 per cent when the shell produced strong and narrow lines.

2. The hydrogen lines do not show the effect clearly:  $H_9$ ,  $H_{10}$ , and  $H_{11}$  were unaffected by the disappearance of the shell, but in the wings of  $H\delta$  the change was in the same direction as in the lines of  $O\ II$  and  $Si\ IV$ . Why the wings of the higher members of the Balmer series fail to show the effect is not known, but it is reasonable to suppose that because of the prominence of  $H$  in the shell and because of the weakness of the wings of the higher members in the reversing layer there may be complications which do not exist in the case of  $O\ II$  and  $Si\ IV$ . Adopting the formula<sup>44</sup>

$$\frac{H'}{H} = 1 - \frac{\sqrt{3} \eta}{2 \left\{ \left[ 1 + \eta + \frac{\sqrt{3}(1 + \eta)}{2} \right] \sinh \sqrt{3} \tau_r + \left[ \sqrt{1 + \eta} + \frac{\sqrt{3}(1 + \eta)}{2} \right] \cosh \sqrt{3} \tau_r \right\}}$$

which applies to the case of pure scattering, where  $\tau_r$  is the optical thickness of the shell, while  $\eta = \lambda/\kappa$  is the ratio of the absorption coefficient within the line to that of the continuous radiation, in the reversing layer, we find for the undisturbed contour, when  $H'/H = 0.90$ :

$$\eta = 0.25.$$

Three different values of  $\tau_r$  give:

$\tau_r$	$H'/H$
0.1 . . . . .	0.915
.2 . . . . .	.93
0.3 . . . . .	0.95

The observations are best satisfied when  $\tau_r = 0.2$ . This appears entirely reasonable, as to order of magnitude, if we recall that the lines of the shell are strong and that, consequently, the continuous absorption of hydrogen must be appreciable.

In the case of the hydrogen lines the presence of strong absorption lines from the shell must tend to distort at least those parts of the contour where the wings of the sharp line blend with the contour of the broad lines. In the case of emission lines there would be a distortion in the opposite sense, the emission edges tending to fill in the underlying line. It is impossible to allow for these effects numerically.

<sup>43</sup> Struve, *Proc. Nat. Acad. Sci.*, 26, 117, 1940.

<sup>44</sup> *Proc. Nat. Acad. Sci.*, 26, 118, 1940.

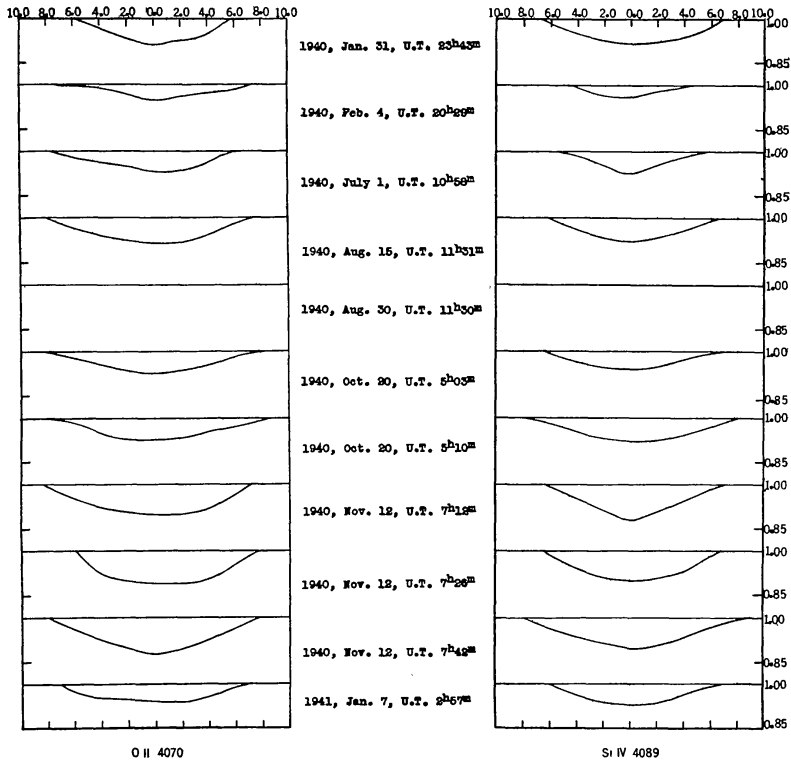


FIG. 3.—Contours of  $O\ II\ 4070$  and  $Si\ IV\ 4089$  in  $\gamma$  Cassiopeiae. Violet is on the right side

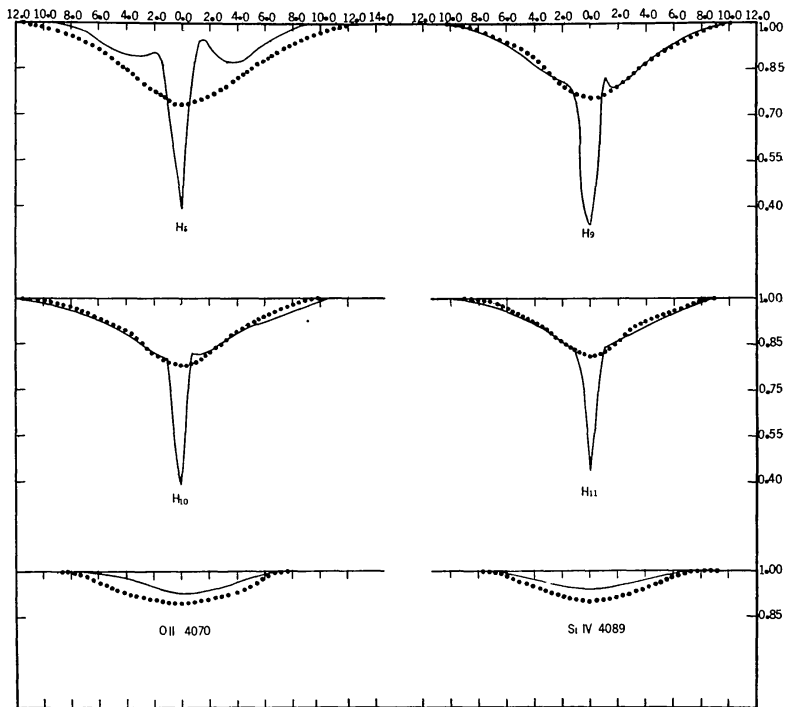


FIG. 4.—The continuous lines represent the mean contours for January 31 and February 4, 1940, when the lines of the shell were strong. The dotted lines represent the mean contours for November 12, 1940, and January 7, 1941, when the lines of the shell were very weak or absent. Violet is on the right side.

14 COMAE BERENICES<sup>45</sup>

Among the B stars several cases are known where rotationally broadened lines occur simultaneously with sharp lines of *H*, *Fe* II, *He* I, etc. These composite spectra do not originate from the accidental overlapping of the images of components in a binary system; they are caused in rapidly rotating stars which are surrounded by tenuous shells of gas whose pressures and thicknesses suggest structures which resemble the reversing layers of supergiant stars. A very remarkable representative of this unusual group of objects, among those of spectral class A, is 14 Comae Berenices, which was described by Morgan in 1932.<sup>46</sup> Morgan found that *Mg* II is very broad and diffuse, while several other lines, notably those of *Ti* II and *Sc* II, are fairly well defined. Among some five hundred bright A-type stars observed at the Yerkes Observatory, Morgan could list only one other star "which possesses a faint, diffuse  $\lambda$  4481 when other lines in the spectrum are narrow." This other star is 17 Leporis, whose spectrum had already been described by Struve and attributed by him to an expanding shell.<sup>47</sup>

Because of the unusual character of the spectrum of 14 Comae we placed it upon our observing program at the McDonald Observatory and obtained the following spectrograms:

Plate	Date	Mid-Exp. U.T.	Dispersion	Emulsion	Spectral Region
CQ 593...	1941, Jan.	8	40 A/mm at $\lambda$ 3933	Eastman Process	$\left\{ \begin{array}{l} \lambda\lambda\ 3300-4700 \\ 3600-4600 \\ 3280-4900 \end{array} \right.$
CQ 604...		9			
CQ 614...		11			
CG 615...		13	30 A/mm at $\lambda$ 4500	{ Process film	$\left\{ \begin{array}{l} 3700-4900 \\ 3700-4900 \end{array} \right.$
CG 616...		13			
CG 617...		14		{ Agfa Super Pan Press	$\left\{ \begin{array}{l} 3900-6600 \\ 3900-6600 \end{array} \right.$
CG 618...		14			

The material obtained at the Yerkes Observatory contains, in addition to the spectrograms discussed by Morgan, a number of excellent Process plates taken in 1932, 1933, and 1934 and covering the region  $\lambda\lambda$  4000-4700 with a dispersion of 30 A/mm at  $\lambda$  4500. The photographic region has already been described by Morgan. Plate IX is a reproduction of our spectrogram CG 616. There are several faint broad lines which had not been recorded by Morgan, but they show nothing unusual and clearly belong to a normal late A-type star whose lines have been greatly broadened by rotation and whose strong wings of the hydrogen lines give evidence of strong Stark effect and hence of low luminosity. The star is a member of the Coma cluster and as such belongs to the main sequence.

There has apparently been no change in the spectrum during the last nine years: our new spectrograms CG 615 and 616 match almost exactly those taken at the Yerkes Observatory.

The spectra taken in the ultraviolet region differ greatly from those taken in the photographic region: they show a large number of sharp lines, and the rotationally broadened lines are weak or absent. This is partly due to the fact that *Fe* II, which is principally responsible for the diffuse lines, abounds in the photographic region but is quite infrequent between  $\lambda$  3300 and  $\lambda$  3700. But we shall see that the effect is enhanced by the continuous Balmer absorption of the reversing layer, which cuts down the rotationally broadened lines but does not affect the sharp lines originating in the shell.

That we are actually dealing with a shell will be shown in the discussion of *H*, *Mg*, *Si* II, etc.

<sup>45</sup> BS 4733,  $\alpha$  21<sup>h</sup>24<sup>m</sup>0,  $\delta$  +27°29' mag. 5.15, sp. A5.

<sup>46</sup> *Ap. J.*, 76, 144, 1932.

<sup>47</sup> *Ap. J.*, 72, 343, 1930; 76, 85, 1932; *Pub. Yerkes Obs.*, 7, Part I, 28, 1929.

Table 4 gives a list of lines between  $\lambda$  3287 and  $\lambda$  3945 which we have measured in the spectrum of  $\epsilon$  Comae, together with those measured on a recent plate of  $\epsilon$  Aurigae. It is convenient to compare  $\epsilon$  Comae with this cF2 supergiant, as well as with the cA2 supergiant  $\alpha$  Cygni. The ultraviolet wave lengths of the latter have already been published.<sup>48</sup> The new list of  $\epsilon$  Aurigae is an extension of former lists made at the Yerkes Observatory for the photographic region.<sup>49</sup> The identifications are those for  $\epsilon$  Aurigae. They should be considered in the light of the notes at the end of Table 4, which also refer to the spectrum of  $\epsilon$  Aurigae. With the help of these notes it is in many cases possible to decide to what extent a blend may be serious. But it must be remembered that the correlation between laboratory intensities of any given element and stellar intensities is not exact.

We proceed with a detailed description of the spectrum. The shell may best be compared with  $\epsilon$  Aurigae (cF2), which it resembles more than  $\alpha$  Cygni (cA2). Most of the metallic lines of  $\epsilon$  Comae are much weaker than those of  $\epsilon$  Aurigae, but a few of the most intense ultraviolet lines of  $Ti$  II and the lines H and K of Ca II are stronger in  $\epsilon$  Comae.

*H*.—With the exception of  $H\alpha$  the Balmer lines are broadened and very diffuse. This broadening is caused by Stark effect, and the lines must originate in the A-type reversing layer. This is the only known case of a shell which is not conspicuous by its sharp lines of *H*. In order to test the occurrence of *H* in the shell, two spectrograms were taken in the visual region. Plate IX shows that  $H\alpha$  is narrow and sharp. It must belong to the shell. The last Balmer line in  $\epsilon$  Comae is  $H_{18}$ . Referring to the diagram by Unsöld and Struve,<sup>50</sup> we infer that for spectral type A5, of the reversing layer, the corresponding luminosity must be low and the star must belong to the main sequence.<sup>51</sup> The relative weakness of *H* in the shell shows that the temperature of the exciting radiation is low.

*He*.—There is no *He* in the shell. A faint, broad absorption feature at  $\lambda$  4025 could perhaps be the triplet line  $\lambda$  4026. But  $\lambda$  4472 and  $D_3$  are definitely missing in the reversing layer. Hence we conclude that the spectral class of the reversing layer is A.

*Na I*.—The lines  $D_1$  and  $D_2$  are strong and sharp. They must come from the shell, and their great intensity shows that the ionization is moderate and that the exciting temperature is low. The excitation potential is 0, and the ionization potential is 5.1 v.

*Mg I*.—The triplet  $\lambda\lambda$  3829, 3832, and 3838, which is present in Pleione<sup>52</sup> and  $\epsilon$  Leporis<sup>53</sup> is not definitely observed in  $\epsilon$  Comae. This may be due to overlapping with the strong wings of  $H_9$ , in the case of  $\lambda$  3832 and  $\lambda$  3838; but  $\lambda$  3829 is also absent in  $\epsilon$  Comae, although it is fairly strong in  $\alpha$  Cygni and  $\epsilon$  Aurigae. The lines  $\lambda$  3829 and  $\lambda$  3838 come from metastable levels. The excitation potential is 2.7 v., and the ionization potential is 7.6 v. The stellar line  $\lambda$  4572 is probably entirely due to  $Ti$  II, and the *Mg I* inter-system line  $\lambda$  4571.10 is absent. The triplet  $\lambda\lambda$  5167, 5173, and 5184 is not in the best region of the spectrograms and has not been observed.

*Mg II*.—The line  $\lambda$  4481 is present only in the reversing layer, as a very diffuse and shallow band whose rotational broadening corresponds to about 200 km/sec. This fixes the spectral class of the reversing layer at about A5. The complete absence of *Mg II* in the shell is in harmony with the evidence from other shells and has been explained as a result of dilution.<sup>54</sup>

<sup>48</sup> O. Struve, *Ap. J.*, **90**, 699, 1939.

<sup>49</sup> Frost, Struve, and Elvey, *Pub. Yerkes Obs.*, **7**, Part II, 1932; W. W. Morgan, *Pub. Yerkes Obs.*, **7**, Part III, 1935.

<sup>50</sup> *Ap. J.*, **91**, 365, 1940.

<sup>51</sup> This is similar to our conclusion in regard to another shell star, Pleione: *Ap. J.*, **93**, 446, 1941.

<sup>52</sup> *Ibid.*

<sup>53</sup> *Ap. J.*, **90**, 730, 1939.

<sup>54</sup> Struve and Wurm, *Ap. J.*, **88**, 84, 1938.



TABLE 4  
ABSORPTION LINES OF  $\epsilon$  AURIGAE AND I4 COMAE

$\epsilon$ AURIGAE		I4 COM. BER.		IDENTIFICATION IN $\epsilon$ AURIGAE
$\lambda$	Int.	$\lambda$	Int.	
3287	5	.86	3	<i>Ti</i> II .67 (40)
3295	6	.67	4	<i>Fe</i> II .81 (6), <i>Fe</i> II .24 (4), <i>Cr</i> II .42 (30)
3303	7	.16	3n	<i>Fe</i> II 2.86 (4), <i>Na</i> I 2.98 (8)
3308.83	3	.68	2	<i>Ti</i> II .82 (8)
3310.82	3	.....	.....	<i>Cr</i> II .65 (18)
3312.02	4	.37	I	<i>Cr</i> II 1.93 (20), <i>Cr</i> II 2.18 (18)
3312.92	0	.....	.....	<i>Fe</i> II .71 (1), <i>Cr</i> II .08 (7)
3313.96	2	4.52	In	{ <i>Fe</i> II .00 (1), <i>Cr</i> II .06 (1), <i>Cr</i> II .57 (15)
3315.53	3			
3318.02	3	.13	3	<i>Ti</i> II .03 (10)
3319.18	I	.....	.....	<i>Ti</i> II .08 (1)
3321.68	4	.57	2	<i>Ti</i> II .71 (25), ( <i>V</i> II .54 (150))
3322.86	3	3.00	4	<i>Ti</i> II .93 (75), <i>Fe</i> II 3.07 (8)
3323.53	0	.....	.....	<i>Ti</i> II .40 (pr), <i>Cr</i> II .53 (3), <i>Fe</i> I .75 (7)
3324.33	3	.24	I	<i>Cr</i> II 4.06 (20), <i>Cr</i> II 4.34 (12)
3326.83	4	.96	2	<i>Ti</i> II .78 (20)
3328.30	3	.33	I	<i>Cr</i> II .35 (12), ( <i>Fe</i> II 9.07 (2))
3329.58	4	.65	4	<i>Ti</i> II .44 (70)
3330.69	0	.....	.....	( <i>Sc</i> II 1.09 (3))
3332.10	5	.23	2	<i>Ti</i> II .11 (30)
3335.21	6	.20	3	<i>Ti</i> II .17 (40), <i>Cr</i> II .28 (30)
3336.34	4	.51	I	<i>Cr</i> II .33 (35), ( <i>Mg</i> I .60 (20))
3337.71	3	.....	.....	<i>Ti</i> II .85 (2), <i>V</i> II .84 (200)
3338.50	2	.....	.....	<i>Fe</i> II .52 (3)
3339.77	3	0.08	4	{ <i>Si</i> II .89 (3), <i>Cr</i> II .80 (50)
3340.47	3			
3341.79	5	2.01	3	<i>Ti</i> II .84 (100)
3342.36	2	.79	2	<i>Cr</i> II .51 (50)
3343.69	3	.86	3	<i>Ti</i> II .78 (10)
3344.69	0	.....	.....	<i>Zn</i> I .94 (10)
3346.68	4	.57	2	<i>Ti</i> II .73 (15)
3347.85	3	.05	I	<i>Cr</i> II .83 (30)
3349.11	ION	.28	6	<i>Ti</i> II .46 (125), <i>Ti</i> II .00 (75), ( <i>Ti</i> II 8.91 (10))
3350.56	I	.....	.....	<i>Ti</i> II .51 (1)
3351.86	2	2.29	on	<i>Ti</i> II 2.07 (5)
3353.60	3n	.70	2	<i>V</i> II 3.78 (30), ( <i>Ti</i> II 4.64 (60)), <i>Sc</i> II .74 (20)
3355.94	2	6.05	0	<i>Fe</i> II .26 (2), <i>Zr</i> II .10 (18)
3357.39	3	.17	0	( <i>Fe</i> II .96 (0)), ( <i>Cr</i> II .40 (4))
3358.40	3	.58	2	<i>Fe</i> II .25 (3), <i>Cr</i> II .50 (75)
3359.82	2n	0.15	In	<i>Fe</i> II .10 (3), <i>Cr</i> II .30 (100), ( <i>Ti</i> II .12 (pr), <i>Fe</i> II .31 (0))
3361.11	5	.45	7n	{ <i>Ti</i> II .19 (125)
3361.97	2			
3362.72	0	.....	.....	{ <i>Sc</i> II .95 (8), ( <i>Ca</i> I 2.00 (35))
3363.79	2	.....	.....	<i>Ti</i> II .65 (1)
3364.52	0	.60	I	( <i>Sc</i> II .52 (1)) ( <i>Cr</i> II 3.71 (6))
3365.17	0	.....	.....	<i>Fe</i> I .52 (5)
3366.25	2	5.99	In	<i>Fe</i> II .64 (0), <i>Fe</i> II .41 (1)
3368.07	4n	.07	3	<i>Ti</i> II .18 (8)
3369.12	5n	8.93	In	<i>Cr</i> II .05 (150), ( <i>Fe</i> II .63 (0))
3370.78	0	.35	0	<i>Fe</i> II .35 (3), ( <i>Ti</i> II .22 (2))
3372.55	15n	.55	10	<i>Fe</i> I .80 (10)
				<i>Ti</i> II .77 (100), ( <i>Ti</i> II .23 (10))

TABLE 4—Continued

ε AURIGAE		14 COM. BER.		IDENTIFICATION IN ε AURIGAE
λ	Int.	λ	Int.	
3374.34	4n	.44	on	<i>Ti</i> II .35 (8), ( <i>Ni</i> II 3.08 (4))
3376.44	2n			<i>Cr</i> II .72 (3), <i>Cr</i> II .27 (5)
3377.41	1			<i>Cr</i> II .36 (2)
3378.48	2	.20	1	<i>Cr</i> II .34 (20), <i>Fe</i> I .69 (6)
3379.66	2			{ <i>Cr</i> II .82 (60), ( <i>Ti</i> II .92 (1)), ( <i>Sc</i> II .42 (3))
3380.32	4	.22	8	
3381.53	0			( <i>Fe</i> II 1.00 (4))
3382.74	4	.96	2	<i>Cr</i> II .68 (60)
3383.79	6	4.00	4	<i>Ti</i> II .77 (125)
3385.29	0			
3386.10	0			<i>Fe</i> II .45 (1)
3387.80	8			{ <i>Ti</i> II .85 (50), ( <i>Fe</i> II 8.13 (2))
3388.56	3	.81	4	
3391.43	3	.81	2	<i>Cr</i> II .42 (60), ( <i>Fe</i> II .30 (1)), ( <i>Zr</i> II .97 (100))
3392.13	2			<i>Fe</i> I .62 (15)
3393.02	1			{ <i>Cr</i> II 3.00 (25), <i>Ni</i> I 2.08 (100); ( <i>V</i> II 2.66 (50))
3393.79	0	.44	in	
3394.49	4	.51	5	<i>Ti</i> II .55 (40)
3398.39	in	.72	on	<i>Fe</i> II .36 (4)
3399.58	2			<i>Cr</i> II .54 (10), <i>Fe</i> I .36 (15)
3401.59	0			<i>Fe</i> I .53 (6), ( <i>Ni</i> II .77 (2))
3402.59	2	.30	on	<i>Ti</i> II .42 (8), ( <i>Cr</i> II .43 (20))
3403.53	4	.34	3	<i>Cr</i> II .32 (100)
3405.11	1			( <i>Ti</i> II 4.96 (1))
3407.36	3n	.17	2	<i>Ti</i> II .21 (3), <i>Fe</i> I .46 (20), <i>Ni</i> II .32 (8)
3408.92	5	.81	4	<i>Cr</i> II .77 (150)
3410.07	3	.18	2	<i>Ti</i> II 9.82 (4), ( <i>Zr</i> II .25 (20))
3411.93	0			
3413.45	1	.96	on	<i>Fe</i> I .14 (15), ( <i>V</i> II 4.19 (10))
3414.81	2	.80	1	<i>Ni</i> I .78 (150), ( <i>Fe</i> II .14 (2))
3415.99	2	6.07	on	<i>Fe</i> II 6.02 (5)
3417.10	0			<i>Ti</i> II 6.96 (2), ( <i>Fe</i> I .87 (12))
3418.73	0			<i>Fe</i> I .52 (10)
3419.81	0			<i>Fe</i> II 0.18 (0)
3421.30	6	.07	4	<i>Cr</i> II .20 (75), ( <i>Cr</i> II .62 (4))
3422.90	5	.77	5	<i>Cr</i> II .74 (125)
3423.92	1			<i>Fe</i> I .30 (10)
3425.73	2	.75	in	<i>Fe</i> II .58 (3)
3427.10	1			{ <i>Fe</i> I .13 (20)
3428.57	1	7.90	0	{ <i>Cr</i> II .94 (6)
3430.65	2	.50	0	<i>Zr</i> II .54 (30)
3432.54	0			
3433.40	6	.35	6	<i>Cr</i> II .30 (75)
3436.11	2n	.18	0	<i>Fe</i> II .11 (5)
3437.09	1			<i>Zr</i> II .15 (10), ( <i>Fe</i> I .06 (3))
3438.33	4	.49	3n	<i>Zr</i> II .24 (100)
3439.03	3			<i>Mn</i> II 8.96 (3)
3440.90	4	.73	1	<i>Fe</i> I .63 (150), <i>Fe</i> I 1.02 (75)
3442.19	7	.12	5	<i>Mn</i> II 1.98 (30), ( <i>Fe</i> II .24 (31)), ( <i>Fe</i> I 2.37 (5))
3443.73	0			<i>Fe</i> I .88 (50), ( <i>Ti</i> II .38 (1))
3444.28	5	.35	5	<i>Ti</i> II .33 (30)
3446.42	3	.42	1	<i>Co</i> II .40 (100), ( <i>K</i> I .72 (8)), ( <i>Ni</i> I .27 (100))
3448.40	on			<i>Fe</i> II .43 (1), ( <i>Y</i> II .79 (10))

## PECULIAR STARS

309

TABLE 4—Continued

ε AURIGAE		14 COM. BER.		IDENTIFICATION IN ε AURIGAE
λ	Int.	λ	Int.	
3450.77	0	.....	.....	<i>Fe I</i> .34 (10), ( <i>Fe II</i> 1.31 (2)), ( <i>Fe II</i> 1.22 (2))
3452.64	3	.27	in	<i>Ti II</i> .48 (4), <i>V II</i> 3.09 (90)
3454.25	2	.....	.....	( <i>Cr II</i> 4.98 (25))
3456.40	3n	6.05	I	<i>Ti II</i> .40 (20), <i>Fe II</i> .93 (5)
3457.56	0	.....	.....	<i>V II</i> .15 (300), <i>Cr II</i> .62 (25)
3458.63	2	.41	I	<i>Ni I</i> .47 (125), <i>Fe I</i> .31 (4), ( <i>Cr II</i> 9.29 (18))
3460.31	6	.37	6	<i>Mn II</i> .32 (20)
3461.57	5	.50	6	<i>Ti II</i> .50 (20)
3462.97	1	.....	.....	<i>Zr II</i> 3.02 (35), ( <i>V II</i> 3.08 (4))
3464.23	2	3.85	0	<i>Fe II</i> .50 (3), ( <i>Sr II</i> .48 (50))
3465.75	4	.71	I	<i>Ti II</i> .65 (3), <i>Fe I</i> .88 (60)
3467.33	1	.37	0	( <i>Cr II</i> .14 (....))
3468.73	3	.....	.....	{ <i>Fe II</i> .68 (8)
3469.64	0}	9.13	0	{ <i>V II</i> .53 (50), <i>Fe II</i> 0.24 (1), ( <i>V II</i> 0.26 (20))
3471.33	3	.....	.....	<i>Fe I</i> .36 (6), ( <i>Cr II</i> 2.07 (15))
3472.61	2	.....	.....	( <i>Fe II</i> .89 (0)), ( <i>Ni I</i> .55 (70))
3474.18	6	3.89	4	<i>Mn II</i> 3.97 (8), <i>Mn II</i> 4.15 (8)
3475.46	4	.83	2	<i>Fe I</i> .46 (70), <i>Cr II</i> .13 (10), ( <i>V II</i> 6.25 (20)), ( <i>Fe I</i> .67 (6))
3477.19	6}	.....	.....	{ <i>Ti II</i> .19 (15), <i>V II</i> .51 (40)
3478.56	0}	.11	4	{ <i>V II</i> .96 (6)
3479.19	0}	.....	.....	{ <i>Zr II</i> .39 (30)
3479.82	2}	.94	I	{ <i>Fe II</i> .91 (2), <i>V II</i> .84 (80)
3481.19	2	.....	.....	<i>Zr II</i> .16 (35)
3482.95	5	.91	3	<i>Mn II</i> .91 (12), ( <i>Cr II</i> .58 (....))
3484.11	2}	.....	.....	{ <i>Cr II</i> .15 (10), ( <i>Fe II</i> .35 (1))
3485.94	2}	4.70	on	{ <i>V II</i> .92 (250), ( <i>Fe II</i> .73 (1))
3488.04	0	.....	.....	<i>Fe II</i> 7.99 (3)
3488.73	4	.72	3	<i>Mn II</i> .86 (10)
3489.88	3	.96	I	( <i>Ti II</i> .75 (2))
3491.10	5	.10	4	<i>Ti II</i> .06 (10), <i>Fe I</i> 0.60 (100)
3493.31	4n	.22	I	<i>Fe II</i> .47 (10), <i>V II</i> .16 (150), <i>Ni I</i> 2.98 (150)
3494.74	I	.98	0	<i>Fe II</i> .67 (5)
3495.97	5	.....	.....	{ <i>Mn II</i> .84 (7), ( <i>Fe II</i> .62 (4)), ( <i>V II</i> 6.09 (80))
3496.85	2n}	6.05	3	{ <i>V II</i> 7.03 (200), ( <i>Fe II</i> 6.34 (0)), ( <i>Fe I</i> 7.10 (10))
3497.68	5}	.51	I	{ <i>Mn II</i> .53 (6), <i>Fe I</i> .84 (40), <i>Zr II</i> .90 (12), ( <i>V II</i> .39 (4))
3500.39	3	.22	I	<i>Ti II</i> .34 (2)
3501.92	2	.....	.....	( <i>Co II</i> .73 (200))
3503.59	2	.....	.....	<i>Fe II</i> .47 (2)
3505.01	8}	4.58	3n	{ <i>Ti II</i> 4.88 (80), <i>V II</i> 4.43 (400)
3505.63	2}	.....	.....	{ <i>Zr II</i> .49 (15), <i>Zr II</i> .67 (12), ( <i>Ti II</i> .90 (tr))
3507.49	2	.68	0	<i>Fe II</i> .39 (3)
3508.17	I	.....	.....	<i>Fe II</i> .21 (1)
3509.82	I	.....	.....	<i>Ti II</i> .85 (3)
3510.85	5	.60	3	<i>Ti II</i> .85 (60)
3511.93	4	.....	.....	<i>Cr II</i> .84 (30)
3512.88	0	.....	.....	<i>Fe II</i> .72 (2), <i>Ti II</i> 3.06 (tr), <i>Cr II</i> 3.05 (10)
3513.98	3}	4.41	2n	{ <i>Fe I</i> .83 (30), <i>Ni II</i> .93 (8), <i>V II</i> 4.42 (20)
3515.15	2}	.....	.....	{ <i>Fe II</i> .82 (2), <i>Ni I</i> .07 (150)
3516.49	0	.....	.....	<i>Fe I</i> .41 (5), ( <i>V II</i> .00 (5))
3517.40	4	.32	I	<i>V II</i> .30 (800)
3518.49	I	.....	.....	( <i>Cr II</i> .65 (2))

TABLE 4—Continued

$\epsilon$ AURIGAE		14 COM. BER.		IDENTIFICATION IN $\epsilon$ AURIGAE
$\lambda$	Int.	$\lambda$	Int.	
3520.24	4	.43	2	<i>Ti</i> II .26 (20), <i>V</i> II .02 (120)
3520.76	1	.....	.....	<i>Zr</i> II .85 (5)
3521.58	2	.66	1	<i>V</i> II .84 (90)
3524.62	4	.48	3	<i>V</i> II .71 (200), <i>Ni</i> I .54 (200)
3526.25	3	.43	1	<i>Fe</i> I .04 (20), <i>Fe</i> I .17 (15), <i>Fe</i> I .48 (4), ( <i>Fe</i> I .26 (3))
3529.10	0	.....	.....	( <i>Cr</i> II .73 (2), ( <i>Fe</i> I .82 (6))
3530.82	3	.87	2	<i>V</i> II .76 (500), ( <i>V</i> II 1.48 (10))
3532.08	1	3.08	1	<i>Fe</i> II .65 (2), <i>Fe</i> I 3.20 (10)
3533.87	1	4.19	0	<i>Ti</i> II .86 (2)
3535.58	5	.35	2	<i>Ti</i> II .41 (40), <i>Sc</i> II .73 (15)
3536.44	1	.....	.....	<i>Fe</i> I .57 (15)
3538.08	in	.07	0	<i>V</i> II .24 (50), ( <i>Mg</i> II 8.86 (6))
3539.27	0	.....	.....	<i>Fe</i> II .55 (3)
3541.03	1	.08	on	<i>Fe</i> I .10 (15), <i>V</i> II .34 (50)
3542.37	1	.....	.....	<i>Fe</i> I .09 (15), <i>Zr</i> II .63 (25), ( <i>V</i> II .48 (4))
3544.20	0	.....	.....	.....
3545.23	7	.11	1	<i>V</i> II .19 (1000)
3546.88	0	.....	.....	( <i>V</i> II 7.07 (5))
3548.01	1	.....	.....	<i>Mn</i> I .03 (40)
3549.08	2	.....	.....	{ <i>Fe</i> II .03 (1), ( <i>Ti</i> II .24 (pr))
3550.93	0	9.73	on	
3551.90	3	.....	.....	<i>Zr</i> II .96 (18)
3552.64	1	.77	on	( <i>Fe</i> I .85 (3))
3553.90	0	.....	.....	<i>Fe</i> I .12 (4)
3554.98	2	.....	.....	<i>Fe</i> I .94 (40)
3556.70	6	.57	4	<i>V</i> II .80 (1500), ( <i>Fe</i> I .90 (7))
3558.51	5	.75	3	<i>Sc</i> II .53 (20), <i>Fe</i> I .53 (30)
3560.64	2	.....	.....	<i>V</i> II .59 (90)
3561.75	3	.43	1	<i>Ti</i> II .58 (3), <i>Ti</i> II .90 (1)
3563.12	0	.....	.....	( <i>Cr</i> II .92 (5))
3564.34	1	.....	.....	( <i>Fe</i> II .52 (pr))
3565.37	3	.....	.....	{ <i>Fe</i> I .40 (60), <i>Ti</i> II .30 (3)
3566.17	4	5.72	3n	
3567.69	4	.84	2	<i>Sc</i> II .70 (20)
3568.97	0	.....	.....	<i>Mn</i> I 9.51 (60)
3570.03	4	.28	2	<i>Fe</i> I .14 (100)
3571.61	0	.....	.....	<i>Cr</i> II .39 (3)
3572.53	6	.57	6	<i>Sc</i> II .55 (50), ( <i>Zr</i> II .50 (30))
3573.83	3	.75	1	<i>Ti</i> II .74 (20)
3576.58	9	.40	5	<i>Sc</i> II .35 (30), ( <i>Ti</i> II .38 (0))
3578.05	0	.....	.....	<i>V</i> II 7.86 (20), <i>Cr</i> I 8.64 (200)
3578.63	3	.....	.....	<i>V</i> II .64 (15), ( <i>Ti</i> II .71 (0))
3579.87	0	.....	.....	.....
3581.10	10	.05	5	<i>Fe</i> I .21 (250), ( <i>Sc</i> II 0.93 (20))
3584.53	0	.....	.....	{ <i>Fe</i> I .66 (8), <i>Y</i> II .52 (100)
3585.52	9	5.11	3n	
3587.09	3	.15	1	<i>Ti</i> II .15 (12)
3587.82	1	.....	.....	<i>V</i> II 8.13 (15)
3589.75	5	.....	.....	{ <i>V</i> II .75 (1000), ( <i>Sc</i> II .63 (10))
3590.36	3	0.00	3	
3592.09	4	.02	1	<i>V</i> II .01 (800)
3593.44	4	.45	1	<i>V</i> II .32 (600), <i>Cr</i> I .50 (160), ( <i>Ti</i> II .08 (21))
3594.56	1	.....	.....	<i>Fe</i> I .64 (8)

TABLE 4—Continued

ε AURIGAE		14 COM. BER.		IDENTIFICATION IN ε AURIGAE
λ	Int.	λ	Int.	
3596.17	4	.12	4	Ti II .06 (60), (Ti II .56 (1r))
3597.97	1			
3600.80	3	.90	2n	Y II .74 (300)
3602.14	2			Y II 1.92 (100), (Fe I .55 (3))
3603.82	5	.77	2n	Cr II .80 (30), (Cr II .86 (10))
3605.37	3	.45	on	Cr I .34 (140), Fe I .48 (15)
3606.88	2			Fe I .70 (20)
3608.88	3	.60	2n	Fe I .87 (100)
3610.73	2n	.86	2n	Y II 1.05 (200), (Fe I .17 (20))
3611.98	1			Fe I 2.08 (8), (V II .58 (10))
3613.21	1			Ti II .33 (pr), Cr II .21 (20)
3613.93	8	.67	10	Sc II .81 (100)
3615.06	1			Fe II 4.87 (5)
3617.35	0			Fe I .80 (12), (Cr II .32 (5))
3619.03	4	8.97	4n	V II 8.92 (200), Fe I 8.78 (125), Ni I .40 (150)
3621.47	3	.35	in	Fe II .27 (6), V II .20 (150), Fe I .47 (15), Fe I 2.00 (12)
3623.43	on			Fe I .19 (8)
3624.92	5	.88	2	Ti II .84 (70), Fe II .89 (5), V II 5.61 (50)
3626.31	1			
3627.67	1			V II .71 (60), Ti II .72 (1)
3629.09	1			Y II 8.71 (100)
3630.74	7	.96	9n	Sc II .74 (100)
3631.72	6			Fe II 2.29 (3), Cr II .49 (50), Cr II .72 (25)
3633.27	3	.00	1	Y II .14 (200), Zr II .51 (10)
3635.04	0			Ti II .35 (pr)
3636.88	0			Cr II .44 (pr)
3640.22	0			Fe I .40 (15)
3641.45	5	.27	2	Ti II .34 (100)
3642.93	6	.92	5	Sc II .83 (50)
3645.43	5	.32	4	Sc II .30 (15), (V II .91 (30))
3647.78	4	8.16	1	Fe I .85 (100), (Cr II .38 (5))
3649.30	0			Fe I .51 (12), Fe I .30 (5)
3650.44	1			Cr II .37 (20)
3651.90	4	.40	2	Sc II .80 (20)
		3.54	0	
3655.45	0			Fe I .47 (4)
3658.42	0			(V II .27 (10)), (H <sub>33</sub> 9.42 (...)), (H <sub>34</sub> 8.42 (...))
3659.90	4	.61	in	Ti II .76 (60)
3661.27	1			V II .38 (200), H <sub>31</sub> .22 (...)
3662.34	4	.51	in	Ti II .24 (40), (H <sub>30</sub> .26 (...))
3663.61	1			H <sub>29</sub> .40 (...)
3664.90	3	.48	0	H <sub>28</sub> .68 (...), Y II .62 (150), Ti II .83 (pr)
3666.25	3			H <sub>27</sub> .10 (...), (Ti II .60 (0))
3667.76	3			{H <sub>26</sub> .68 (...)
3669.53	4	8.97	on	{H <sub>25</sub> .47 (...), V II .41 (300)
3671.46	4	.46	on	H <sub>24</sub> .48 (...)
3673.71	4			H <sub>23</sub> .76 (...)
3674.66	2	.88	1	V II .69 (30), Zr II .73 (40)
3676.54	5			H <sub>22</sub> .36 (...)
3677.91	6	.63	3	Cr II .86 (30), (Sc II 8.36 (3))
3679.51	5	.22	1	H <sub>21</sub> .36 (...), Fe I .92 (40), (Ti II .69 (pr))
3682.77	6			H <sub>20</sub> .81 (...)
3685.26	10	.28	10	Ti II .20 (250)
3687.09	8			H <sub>19</sub> 6.83 (...), Fe I 7.47 (40)

TABLE 4—Continued

$\epsilon$ AURIGAE		14 COM. BER.		IDENTIFICATION IN $\epsilon$ AURIGAE
$\lambda$	Int.	$\lambda$	Int.	
3689.54	1	.....	.....	<i>Fe</i> I .47 (12)
3691.54	10	.02	1nn	<i>H</i> <sub>18</sub> .56 (.....)
3694.22	3	.....	.....	<i>Fe</i> I .03 (20), ( <i>Cr</i> II 4.08 (2))
3697.22	12	.08	3nn	<i>H</i> <sub>17</sub> .15 (.....)
3697.87	1	.....	.....	<i>Cr</i> II 8.00 (15), <i>Zr</i> II 8.17 (100)
3700.35	2	.....	.....	<i>V</i> II .34 (200), ( <i>V</i> II .13 (40))
3701.03	1	.....	.....	<i>Fe</i> I .10 (20)
3703.91	10	4.31	3nn	<i>H</i> <sub>16</sub> .86 (.....)
3706.06	15	5.55	4	<i>Ca</i> II .04 (10), <i>Fe</i> I 5.58 (100), ( <i>Ti</i> II .22 (20))
3707.88	3	.....	.....	<i>Fe</i> I .83 (20)
3709.26	4	.....	.....	<i>Fe</i> I .26 (75), <i>Zr</i> II .28 (60), ( <i>V</i> II .34 (40))
3710.27	4	.45	4n	<i>Y</i> II .29 (500)
3711.61	20	.....	.....	<i>H</i> <sub>15</sub> .97 (.....)
3712.63	20	.55	4nn	<i>Cr</i> II .97 (40)
3715.56	15	.....	.....	<i>V</i> II .47 (1200), <i>Cr</i> II .19 (20), <i>Cr</i> II .45 (18)
3718.32	2	.....	.....	<i>V</i> II .16 (60)
3719.96	5	20.05	3	<i>Fe</i> I .95 (250)
3721.91	20	.88	6	<i>H</i> <sub>14</sub> .94 (.....), ( <i>Ti</i> II .64 (15))
3723.96	3	.....	.....	<i>Ti</i> II 4.09 (1)
3725.49	1	.....	.....	<i>Fe</i> II .30 (3)
3727.86	10	.35	2n	<i>V</i> II .35 (1000), <i>Fe</i> I .64 (50), <i>V</i> II 8.34 (200)
3730.89	0	.....	.....	<i>Zr</i> II .26 (35)
3732.86	5	3.19	2	<i>V</i> II .76 (800), ( <i>Fe</i> I 3.33 (40))
3734.60	16	.86	10n	<i>H</i> <sub>13</sub> .37 (.....), <i>Fe</i> I .88 (300)
3736.95	10	.83	5	<i>Ca</i> II .92 (11), <i>Fe</i> I 7.14 (150)
3738.36	3	.....	.....	<i>Cr</i> II .38 (15), <i>Fe</i> I .31 (10)
3739.74	1	.....	.....	( <i>Fe</i> I .53 (3))
3741.62	7	.64	3	<i>Ti</i> II .65 (50)
3743.35	5	.....	.....	<i>V</i> II .61 (40)
3745.68	8	.....	.....	{ <i>V</i> II .81 (800), <i>Fe</i> I .58 (100)
3746.33	2	.93	4	{ <i>Zr</i> II 5.97 (40)
3748.23	6	.....	.....	{ <i>Fe</i> I .27 (60), <i>Ti</i> II .00 (10), <i>Fe</i> II .49 (8),
3750.37	25	9.66	15n	{ <i>Cr</i> II .68 (5)
3753.43	0	.....	.....	{ <i>H</i> <sub>12</sub> .15 (.....), <i>Fe</i> I 9.50 (200), ( <i>V</i> II .88
3754.62	4	.....	.....	{(600)}
3757.87	7	.97	1	<i>Fe</i> I .62 (8)
3759.51	6	.14	8	<i>Cr</i> II .59 (12)
3761.54	8	.36	6	<i>Ti</i> II .69 (30), <i>Fe</i> I 8.25 (150)
3763.91	5	.80	1	<i>Ti</i> II .30 (200)
3765.57	3	.....	.....	<i>Ti</i> II .32 (200), ( <i>Ti</i> II .88 (15)), ( <i>Cr</i> II .90
3767.05	4	.....	.....	(4), ( <i>Cr</i> II .69 (4))
3769.67	4	.....	.....	<i>Fe</i> I .80 (100)
3770.64	7	.30	15n	<i>Cr</i> II .62 (8)
3772.72	1	.....	.....	<i>Fe</i> I .21 (80), <i>Zr</i> II .82 (25), ( <i>Cr</i> II 6.65 (2))
3774.52	3	4.06	3	<i>Ni</i> II .46 (5), ( <i>Fe</i> I 0.00 (4))
3776.22	4	6.70	2	<i>H</i> <sub>11</sub> .63 (.....), ( <i>Ti</i> II .42 (11)), ( <i>V</i> II .97
3778.42	2	.....	.....	{(400)}
3779.68	2	.....	.....	<i>V</i> II .96 (80)
3781.60	1	.....	.....	<i>Ti</i> II .65 (2), <i>Y</i> II .33 (300)
3783.31	5	2.14	1n	<i>Ti</i> II .06 (6), ( <i>Y</i> II .56 (75))
3786.33	4	.....	.....	<i>V</i> II .36 (100)
3787.84	2	.....	.....	( <i>Fe</i> I .43 (3))
				{ <i>Fe</i> II .51 (1)
				{ <i>Fe</i> II .35 (4)
				<i>Ti</i> II .33 (2), ( <i>Fe</i> I .68 (8))
				<i>Fe</i> I .89 (50), ( <i>V</i> II .24 (150))

## PECULIAR STARS

313

TABLE 4—Continued

ε AURIGAE		14 COM. BER.		IDENTIFICATION IN ε AURIGAE
λ	Int.	λ	Int.	
3788.63	2	.34	3n	<i>Y</i> II .70 (200)
3790.09	1			<i>Fe</i> I .10 (12)
3791.43	0			
3794.96	4	5.23	2	<i>Fe</i> I 5.01 (60)
3797.76	20	8.31	20n	<i>H</i> <sub>10</sub> .90 ( . . . )
3799.56	3			<i>Fe</i> I .56 (50), <i>Ti</i> II .79 (tr)
3801.80	1			( <i>Fe</i> I .68 (3))
3803.41	0			<i>Fe</i> II .05 (0)
3805.40	1			<i>Fe</i> I .35 (12)
3807.08	2	6.98	3n	<i>Fe</i> I 6.72 (10), <i>Fe</i> I 7.55 (7)
3809.08	1			( <i>Fe</i> I 8.74 (4))
3810.48	1			
3813.21	8			{ <i>Fe</i> I 2.96 (40), <i>Ti</i> II .40 (2), ( <i>Fe</i> I .08 (5))
3814.65	6	4.29	8n	<i>Ti</i> II .60 (4)
3815.98	5			<i>Fe</i> I .85 (100), ( <i>Fe</i> I .35 (4))
3818.17	1			<i>Y</i> II .35 (60)
3820.37	5	.24	3	<i>Fe</i> I .44 (250)
3821.93	3			<i>Fe</i> II .97 (pr), ( <i>Fe</i> II 2.74 (3))
3824.50	5			<i>Fe</i> I .45 (50), ( <i>Fe</i> II .91 (4))
3825.91	4	.83	5n	<i>Fe</i> I .89 (200)
3827.88	4			<i>Fe</i> I .83 (75)
3829.52	4			<i>Mg</i> I .37 (40)
3832.58	6			<i>Mg</i> I .31 (80), ( <i>Y</i> II .89 (100))
3834.34	1			<i>Fe</i> I .24 (100)
3835.73	20			<i>H</i> <sub>9</sub> .39 ( . . . )
3838.40	4			<i>Mg</i> I .30 (100)
3840.79	6	.78	2	<i>Fe</i> I .45 (80), <i>Fe</i> I 1.06 (80)
3843.19	3			<i>Fe</i> I .27 (8), <i>Zr</i> II .06 (30), <i>Mn</i> II 2.98 (1), ( <i>Sc</i> II 3.06 (4))
3845.25	2			( <i>Co</i> I .47 (60))
3847.10	1			<i>V</i> II .32 (100)
3849.84	5			{ <i>Fe</i> I .98 (40)
3850.43	1	50.62	2n	{ <i>Fe</i> I .83 (12), ( <i>V</i> II .41 (7)), ( <i>Mg</i> II .40 (6))
3852.33	0			<i>Fe</i> I .58 (6), ( <i>V</i> II .10 (4))
3853.56	3			<i>Si</i> II .67 (3)
3856.09	6	.27	3	<i>Si</i> II .03 (8), <i>Fe</i> I .38 (50)
3858.22	1			( <i>Ni</i> I .31 (40))
3859.93	5	.93	3	<i>Fe</i> I .92 (300)
3862.71	3			<i>Si</i> II .60 (6)
3863.87	2			<i>Fe</i> II .95 (1), ( <i>Fe</i> II .41 (1)), <i>V</i> II .81 (60)
3865.64	3	.26	2n	<i>Cr</i> II .59 (20), <i>Fe</i> I .54 (30), ( <i>V</i> II .72 (5))
3867.02	2			<i>Fe</i> I .23 (7), ( <i>V</i> II 6.74 (60))
3869.66	1n			<i>Fe</i> I .76 (4), <i>Fe</i> I .56 (3)
3872.56	5	.89	3n	<i>Fe</i> I .51 (60)
3875.75	0			<i>Fe</i> I 6.05 (4), ( <i>V</i> II .67 (5))
3878.56	10	.26	2n	<i>Fe</i> I .58 (100), ( <i>Fe</i> I .03 (60)), ( <i>V</i> II .72 (300))
3880.58	0			<i>Fe</i> II .78 (1)
3882.40	4			( <i>Mn</i> II 3.28 (3))
3884.62	1			<i>V</i> II .85 (50)
3886.64	8			<i>Fe</i> I .30 (40), ( <i>Fe</i> I 7.06 (15))
3889.17	20	8.21	20n	<i>H</i> <sub>8</sub> .05 ( . . . )
3891.70	0			<i>Cr</i> II 2.14 (2), ( <i>Mg</i> I .98 (3))
3893.67	1			<i>Fe</i> I .40 (7)
3895.74	4	.24	1	<i>Fe</i> I .67 (25), ( <i>V</i> II 6.16 (60)), ( <i>Mg</i> I .66 (5))
3897.94	1			<i>Fe</i> I 8.02 (10)
3899.36	1			<i>V</i> II .16 (200), <i>Fe</i> I .72 (30)

TABLE 4—Continued

ε AURIGAE		14 COM. BER.		IDENTIFICATION IN ε AURIGAE
λ	Int.	λ	Int.	
3900.56	7	.13	5	<i>Ti</i> II .54 (70)
3903.04	4	.....	.....	<i>Fe</i> I 2.96 (20), <i>V</i> II .27 (250)
3905.80	6	.59	3n	<i>Cr</i> II .64 (18), <i>Fe</i> I 6.04 (5), <i>Si</i> I .53 (10)
3908.71	0	.....	.....	.....
3909.34	I	.....	.....	<i>Fe</i> I .84 (3)
3911.14	I	.....	.....	.....
3913.63	10	.36	5	<i>Ti</i> II .47 (60)
3914.24	3	.....	.....	<i>V</i> II .33 (250), <i>Fe</i> II .48 (2)
3916.35	3	.....	.....	<i>V</i> II .42 (200)
3918.48	2	.49	I	<i>Fe</i> I .65 (6), ( <i>Fe</i> I .33 (3)), ( <i>Mn</i> I .32 (3))
3920.38	3	.35	I	<i>Fe</i> I .27 (20)
3922.99	3	.....	.....	<i>Fe</i> I .92 (25)
3924.59	I	.....	.....	( <i>Ti</i> I .53 (50))
3926.10	I	.....	.....	<i>Fe</i> I 5.95 (6), ( <i>V</i> II .32 (5)), ( <i>V</i> II .50 (10))
3927.85	2	.....	.....	<i>Fe</i> I .94 (30)
3930.18	3	.....	.....	<i>Fe</i> I .31 (25)
3933.83	30	.....	.....	<i>Ca</i> II .68 (400)
3936.12	2	.....	.....	<i>Fe</i> II 5.94 (6), <i>Zr</i> II .06 (7)
3938.65	6	.....	.....	<i>Fe</i> II .97 (4)
3941.40	1n	.....	.....	<i>Fe</i> I 0.89 (5)
3944.08	2	.....	.....	<i>Al</i> I .02 (10)
3945.18	3	.....	.....	<i>Cr</i> II .11 (....), <i>Fe</i> II .23 (pr)

NOTES TO THE IDENTIFICATIONS OF TABLE 4

*H.* In ε Aurigae the Balmer series extends to  $H_{29}$ . Higher members, up to  $H_{34}$ , appear only as blends. In 14 Comae,  $H_{18}$  is the last hydrogen line measured.

*Na* I. λ 3303 is blended with a line of *Fe* II.

*Mg* I.

Laboratory.....	4	100
Star.....	4	4

*Mg* II. Uncertain in the ultraviolet region, but λ 4481 is strong in ε Aurigae.

*Al* I. λ 3944 is the only line.

*Al* II. Three lines near λ 3587 may contribute to star line *Ti* II 3587.15.

*Si* I. λ 3905 probably contributes to a blend with *Fe* II.

*Si* II.

Laboratory.....	3	6	8
Star.....	3	3	6

*S* II. Absent.

*Cl* II. Absent.

*K* I. λ 3446.72 may be present as a blend with *Co* II and *Ni* I.

*K* II. Absent.

*Ca* I. Several weak lines may contribute slightly to a blend with *Sc* II. But λ 3644 is absent. In the ordinary photographic region λ 4227 is strong.

*Ca* II. Several lines are present:

Laboratory.....	10	400
Star.....	10	30

*Sc* I. Probably absent.

*Sc* II.

Laboratory.....	10	20	50	100
Star.....	3	4	6	7

*Ti* I. λ 3924 (50) may be present. But λ 3653.50 (100) and λ 3642.68 (80) are absent.



## PECULIAR STARS

315

TABLE 4—NOTES—*Continued**Ti* II.

Laboratory.....	pr	tr	1	2	3	4	8	10
Star.....	o	o	o-1	1	2	3	3	3-4
Laboratory.....	15	20	30	40	50	60	80	100
Star.....	4	4	5	5	6	6	7	10

*V* I. Probably absent.*V* II.

Laboratory.....	6	10	15	20	50	80	90	100
Star.....	o	o	o-1	o-1	1	1	2	2
Laboratory.....	200	250	500	600	800	1000	1200	...
Star.....	2-3	3	3	4	5	7	10	...

*Cr* I. Uncertain. Laboratory intensity 200 is about 0 in the star.*Cr* II.

Laboratory.....	1	2	5	7	10	12
Star.....	Obs.	Obs.-o	o	1	2	3
Laboratory.....	15	30	60	100	150	..
Star.....	3	3-4	4	5	5	..

*Mn* I. Quite doubtful.

Laboratory.....	50	60
Star.....	Obs.-o	o

*Mn* II.

Laboratory.....	3	10	20	30
Star.....	4	4	6	7

*Fe* I.

Laboratory.....	4	5	6	8	10	12	15	20
Star.....	o	o	o	o-1	1	1	1	2
Laboratory.....	40	50	75	80	100	200	250	..
Star.....	3	4	4	5	5	5	6	..

*Fe* II.

Laboratory.....	o	1	2	3	4
Star.....	o	o	1	2	2
Laboratory.....	5	6	8	10	..
Star.....	2	2-3	3	4	..

*Co* I.  $\lambda$  3495.1 (150) may contribute to the star line *Ti* II 3404.96, but *Co* I 3453.5 (200) is not present.*Co* II. The strongest lines  $\lambda$  3501.73 (200) is probably present. This line is also present in  $\alpha$  Cyg,  $\eta$  Leo, and  $\alpha$  CVn.*Ni* I. Probably contributes only to blends.*Ni* II. Probably contributes appreciably to several blends, especially to star line  $\lambda$  3769.67.*Zn* I.  $\lambda$  3344.94 (10) is probably present, with stellar intensity 0.*Sr* I. Absent.*Sr* II. Two lines in this region contribute to blends.*Y* I. Absent.*Y* II.

Laboratory.....	60	100	200	300	500
Star.....	1	1-2	2-3	3	4

*Zr* I. The strongest lines are uncertain because of blends.*Zr* II. Most strong lines are blended.

Laboratory.....	5	18	30	100
Star.....	1	1-2	2	4

*Mo* II. Absent.*Ba* II.  $\lambda$  3891.78 (50) may contribute to a blend of stellar intensity 0.*La* II. Because of blends no lines were identified.

*Si II*.—All excited levels of *Si II* are depopulated by the dilution of the radiation. The very faint diffuse feature near  $\lambda 4130$  must come from the reversing layer. The lower levels of these lines and of the group near  $\lambda 3860$  are not metastable. The excitation potentials of the two groups are 9.8 v. and 6.8 v. The ionization potential is 16.3 v. Our observations of Pleione and of  $\gamma$  Cassiopeiae, where the excitation temperatures are high, show conclusively that the weakness of *Si II* and *Mg II* in all shells cannot be attributed to the relatively high excitation potentials of these lines.

*Ca I*.—The ultimate line  $\lambda 4227$  is moderately strong in the shell. In Plate IX a weak diffuse line flanks the *Ca I* line on the violet side. This may be the *Cr II* line  $\lambda 4225$  of the reversing layer. The excitation potential is 0, and the ionization potential is 6.1 v.

*Ca II*.—The lines H and K are exceedingly strong and must belong to the shell. Their excitation potential is 0. The normal, excited lines  $\lambda 3737$  and  $\lambda 3706$  are both blended with strong lines of *Fe I*. However, since *Fe I* is relatively weak, we infer that the excited *Ca II* lines are present, despite the fact that their lower levels are not metastable. They are, however, much weaker in  $\epsilon$  Comae than in  $\epsilon$  Aurigae (see Pl. X), while the reverse is true for H and K. If the excitation temperatures of the two sources are similar, the product of the ratios

$$\frac{3706 (\epsilon \text{ Aur})}{3706 (14 \text{ Com})} \times \frac{3934 (14 \text{ Com})}{3934 (\epsilon \text{ Aur})}$$

suggests a dilution factor of the order of 10. The excitation potentials of the excited lines are 3.1 v. The ionization potential is 11.8 v.

*Sc II*.—All observed lines come from the ground level,  $a^3D$ , or from low metastable levels and are very strong in  $14$  Comae. These lines are also strong in  $17$  Leporis and fairly strong in Pleione.  $\lambda 4246$  has no diffuse underlying line from the reversing layer.

*Ti II*.—The lines of *Ti II* are numerous and strong in the shell. In the photographic region the stronger lines ( $\lambda\lambda 4300, 4308, 4395, 4399, 4444, 4468, 4563, 4572$ , etc.) have broad rotational lines underlying the sharp cores. These broad lines come from the reversing layer, and fix its spectral class at about A5. The strong *Ti II* lines in the ultraviolet region ( $\lambda\lambda 3323, 3349, 3372, 3394, 3462, 3535, 3596$ , etc.) show little or no diffuse underlying absorption, although the contrast of the emulsion used in the ultraviolet region was at least as good as that of the photographic region.

Table 5 lists those *Ti II* lines of Table 4 which are substantially unblended. All lower levels are metastable. The comparison does not include the ordinary photographic region, partly because the *Ti II* lines there are more complicated by the broad underlying absorptions and partly because we had no suitable plates of  $\epsilon$  Aurigae. The multiplets in Table 5 are arranged in the order of increasing excitation potential of the lower level. Within each multiplet the lines are arranged in order of decreasing laboratory intensity.

The table shows the following effects:

1. Within each multiplet the strongest lines are of more nearly similar intensity in the two stars than the weaker lines. Lines of laboratory intensity 70 or more are practically identical in  $\epsilon$  Aur and  $14$  Com. The faintest laboratory lines are much weaker in  $14$  Com. This effect is easily explained as a consequence of the curves of growth:  $14$  Comae presumably has larger turbulent velocities than  $\epsilon$  Aurigae. Since for the latter the curves of growth begin to bend over for lines whose equivalent breadths are of the order of 0.5 A—which in  $\epsilon$  Aurigae corresponds to *Ti II* lines of intermediate strength—we infer that the more turbulent velocity of  $14$  Comae must be greater than 20 km/sec<sup>55</sup> and may be of the order of 30 or 40 km/sec. This estimate agrees with the fact that with sufficient dispersion the lines of the shell are appreciably broadened.

<sup>55</sup> Struve and Elvey, *Ap. J.*, **79**, 435, 1934.

2. Lines of similar laboratory intensity have a tendency to become relatively weaker in  $\epsilon$  Comae as we pass from low to high excitation potentials. This effect is probably

TABLE 5  
UNBLENDED LINES OF  $Ti$  II

MULTIPLY	$\lambda$	E.P.	INTENSITY		
			Lab.	$\epsilon$ Aur	$\epsilon$ Com
$a^4F-z^4G^0$ . . . . .	3361.19	0.05	125	5	7
	3383.77	0.00	125	6	4
	3394.55	0.01	40	4	5
	3409.82	0.03	4	3	2
$b^4F-z^4G^0$ . . . . .	3444.33	0.15	30	5	5
	3461.50	0.13	20	5	6
	3489.75	0.13	2	3	1
	3500.34	0.12	2	3	1
$b^4F-z^4F^0$ . . . . .	3322.93	0.15	75	3	4
	3329.44	0.13	70	4	4
	3326.78	0.11	20	4	2
	3346.73	0.13	15	4	2
	3318.03	0.12	10	3	3
	3343.78	0.15	10	3	3
$a^2F-z^2D^0$ . . . . .	3596.06	0.60	60	4	4
	3573.74	0.57	20	3	1
	3587.15	0.60	12	3	1
	3501.58	0.57	3	3	1
$a^2F-z^2F^0$ . . . . .	3759.30	0.60	200	6	8
	3761.32	0.57	200	8	6
$a^2F-z^2D^0$ . . . . .	3685.20	0.60	250	10	10
$a^2G-z^2G^0$ . . . . .	3900.54	1.12	70	7	5
	3913.47	1.11	60	10	5
$a^2P-z^2P^0$ . . . . .	3366.18	1.23	8	2	1
	3352.07	1.22	5	2	0
$a^2P-z^2S^0$ . . . . .	3641.34	1.23	100	5	2
$b^4P-z^4S^0$ . . . . .	3332.11	1.24	30	5	2
$b^2D-y^2F^0$ . . . . .	3659.76	1.58	60	4	1
	3662.24	1.56	40	4	1
$b^2D-y^2D^0$ . . . . .	3741.65	1.58	50	7	3
	3776.06	1.58	6	4	2
$b^2G-y^2G^0$ . . . . .	3510.85	1.88	60	5	3
	3509.85	1.88	3	1	A*

\* A = absent.

real (although it is complicated by the effect mentioned in [3], below) and suggests that the excitation temperature of the shell of  $\epsilon$  Comae is lower than that of  $\epsilon$  Aurigae. It

1941ApJ.....94..291S

will be recalled that in Pleione<sup>56</sup> the opposite phenomenon appeared in *Fe* II and probably in *Ti* II, when the shell was compared with  $\alpha$  Cygni.

3. The weakness of  $\lambda\lambda$  3641, 3660, and 3662 in 14 Comae may in part be attributed to the excitation phenomenon discussed in (2). But Plate X shows that the weakening of  $\lambda$  3660 and  $\lambda$  3662 is especially conspicuous. These lines lie close to the Balmer limit, but it is difficult to see how continuous hydrogen absorption can produce the observed phenomenon. If our interpretation of the shell of 14 Comae is correct, its hydrogen is very little excited because of the low excitation temperature, and continuous hydrogen absorption in the shell must be inappreciable; there is no noticeable break in the continuous spectrum at  $\lambda$  3647. The continuous absorption of the reversing layer is irrelevant. In  $\epsilon$  Aurigae we should expect, if anything, a weakening of the *Ti* II lines in the region where the Balmer lines are no longer separately visible. The strength of the *Sc* II lines ( $\lambda\lambda$  3643, 3652, etc.) suggests that Balmer absorption is not appreciable. The peculiar weakness of the *Ti* II lines remains a puzzle. The ionization potential of *Ti* II is 13.6 v.

*V* II.—All lines come from low metastable levels and are weak in 14 Comae. The ionization potential is 14.1 v.—almost identical with that of *Ti* II. It is, therefore, difficult to understand why *V* II is weak, while *Ti* II is strong.

*Cr* II.—All lines come from metastable levels having excitation potentials of 2–3 v. and are moderately strong in 14 Comae. The ionization potential is 16.6 v.

*Mn* II.—All lines come from metastable levels  $a^5S$  and  $a^5D$  of excitation potential 1.7 v. and 1.8 v., respectively. They are strong in 14 Comae. The ionization potential is 15.7 v.

*Fe* I.—Many lines, all from metastable levels or from the ground level, are present. Low-level lines—for example,  $\lambda$  3441, e.p. 0.0 v.—are present in the shell of 14 Comae and are perhaps relatively a little stronger than lines of higher excitation potentials—for example,  $\lambda$  3570, e.p. 0.9 v.;  $\lambda$  3764, e.p. 1.0 v.; and  $\lambda$  3816, e.p. 1.5 v. All lines are weak in 14 Comae, but the curve of growth effect described for *Ti* II is unmistakably present. In the ordinary photographic region all *Fe* I lines are broad and diffuse, coming, as they do, from the reversing layer. There is a faint suspicion of a faint, narrow core in  $\lambda$  4045. The marked weakness of *Fe* I in the shell of 14 Comae is difficult to understand. The ionization potential is 7.8 v.

*Fe* II.—These lines are remarkably weak in 14 Comae. In the ordinary photographic region only the strongest— $\lambda\lambda$  4233, 4352, and 4583—have weak narrow cores. The broad rotational lines from the reversing layer are strong. In the ultraviolet region we have observed relatively few lines of *Fe* II, but those that do appear show but little evidence of the rotationally broadened lines. The narrow lines are weak. The lines of low excitation potential ( $\lambda$  3296, e.p. 1.1 v.) are relatively stronger in 14 Comae than the lines of high excitation potential ( $\lambda$  3469, e.p. 4.1 v.). The number of reasonably unblended lines is small, and no further discussion is possible. The disappearance of the rotationally broadened lines in the ultraviolet region is very conspicuous and must be attributed to continuous Balmer absorption in the reversing layer. The effect is, thus, the same as the one which has been observed in several normal A stars.<sup>57</sup> The ionization potential is 16.5 v.

*Ni* II.—These lines are very weak in 14 Comae. The ionization potential is 18.2 v. The lines are strong in Pleione and intermediate in 17 Leporis. The effect must be due to the lower ionization in the shell of 14 Comae.

*Sr* II.—The ultimate lines,  $\lambda$  4078 and  $\lambda$  4215, are very strong in the shell. Since the ionization potential is 11.0 v., we see in this a confirmation of the relatively low ionization of the shell.

<sup>56</sup> *Loc. cit.*

<sup>57</sup> Struve and Sherman, *Ap. J.*, 91, 428, 1940.

*Y II*.—These lines, all from low metastable levels, are fairly strong in  $\epsilon$  Comae. The ionization potential is 12.3 v.

The preceding notes are summarized in Table 6, which should be compared with similar tables for Pleione<sup>58</sup> and  $\epsilon$  Leporis.<sup>59</sup> It is clear that three effects dominate the spectra of these shells:

a) Dilution weakens *Si II* and *Mg II*.

b) Excitation favors low-level lines in  $\epsilon$  Comae, as compared with  $\epsilon$  Leporis, and favors them in  $\epsilon$  Leporis, as compared with Pleione.

c) Ionization is highest in Pleione, intermediate in  $\epsilon$  Leporis, and lowest in  $\epsilon$  Comae.

Except for the effect of dilution, the spectrum of the shell superficially resembles that of a supergiant star of spectral type F, thereby providing another example for the general rule that the shells correspond to later types than the exciting stars. But there are

TABLE 6

ELEMENTS IN ORDER OF DECREASING INTENSITY RATIO:  $\epsilon$  COM/ $\epsilon$  AUR

Element	<i>Ca II</i>	<i>Na I</i>	<i>Sr II</i>	<i>Sc II</i>	<i>Y II</i>	<i>Ti II</i>	<i>Mn II</i>	<i>Cr II</i>
I.P.....	11.8	5.1	11.0	12.8	12.3	13.6	15.7	16.6
Average E.P.....	0-3	0	0	0-0.3	0-1	1	1.8	2-3

Element	<i>V II</i>	<i>Ni II</i>	<i>Fe I</i>	<i>Fe II</i>	<i>Mg I</i>	<i>Si II</i>	<i>Mg II</i>
I.P.....	14.7	18.2	7.8	16.5	7.6	16.3	15.0
Average E.P.....	1	3	0-1	1-4	2.7	7-10	9

many anomalies which make it impossible to locate the shell within the normal two-dimensional spectral classification:

a) The sharp *H* lines are much too weak for class F.

b) The *Fe I* lines are too weak for class F, or later.

c) The *Fe II* lines are too weak for class A, or earlier.

d) The *Ca II* lines H and K suggest late class F, or G, but this is violated by the *Fe I* lines.

e) The exciting radiation seems to be, if anything, of a lower temperature than in  $\epsilon$  Aurigae (cF2), but the spectral class of the reversing layer is estimated to be about A5. This discrepancy may perhaps be due to the uncertainty of the spectral class of the supergiant  $\epsilon$  Aurigae.

f) Some of these anomalies are consistent with the idea that the pressures within the shells are somewhat lower than those of the reversing layers of the supergiant comparison stars ( $\alpha$  Cygni and  $\epsilon$  Aurigae). In our discussion of Pleione we estimated a pressure within the shell of 0.1 bar, while the average pressure in the atmosphere of a red giant is about 1 bar. Hence, we should expect that ionization would be favored in the shells, while excitation is impeded.

YERKES OBSERVATORY  
AND  
MCDONALD OBSERVATORY  
May 1941

<sup>58</sup> *Ap. J.*, **93**, 446, 1941.

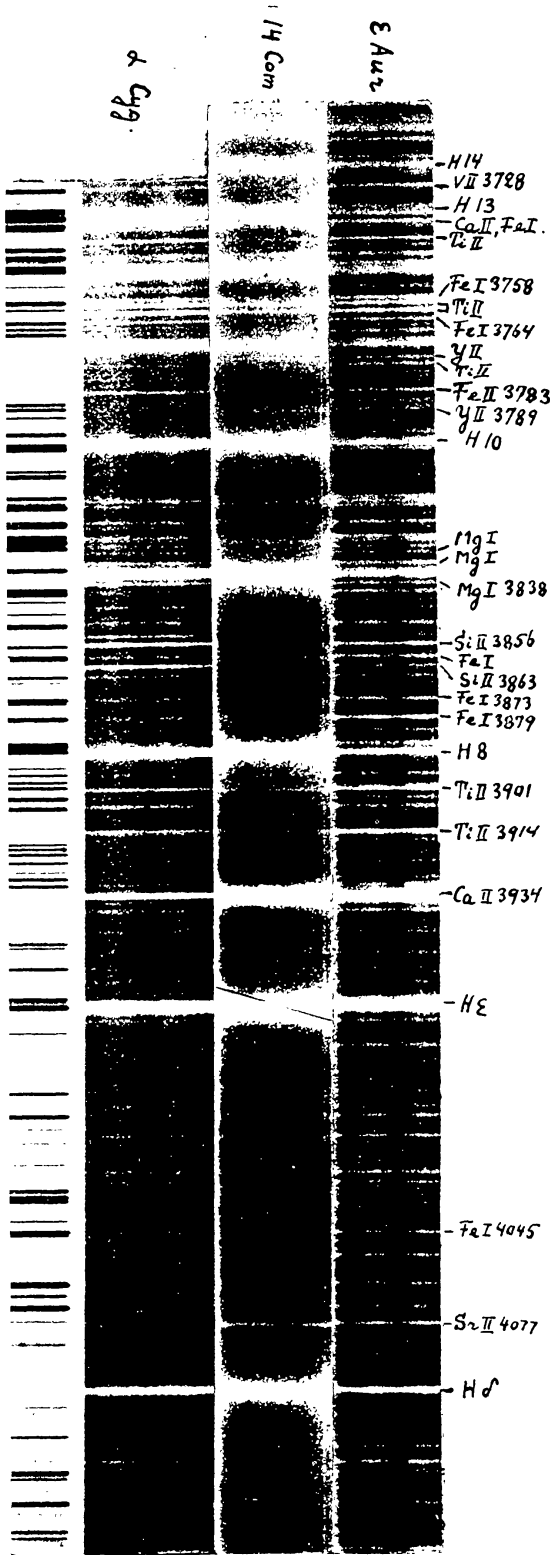
<sup>59</sup> *Ap. J.*, **90**, 734, 1939.

PLATE IX



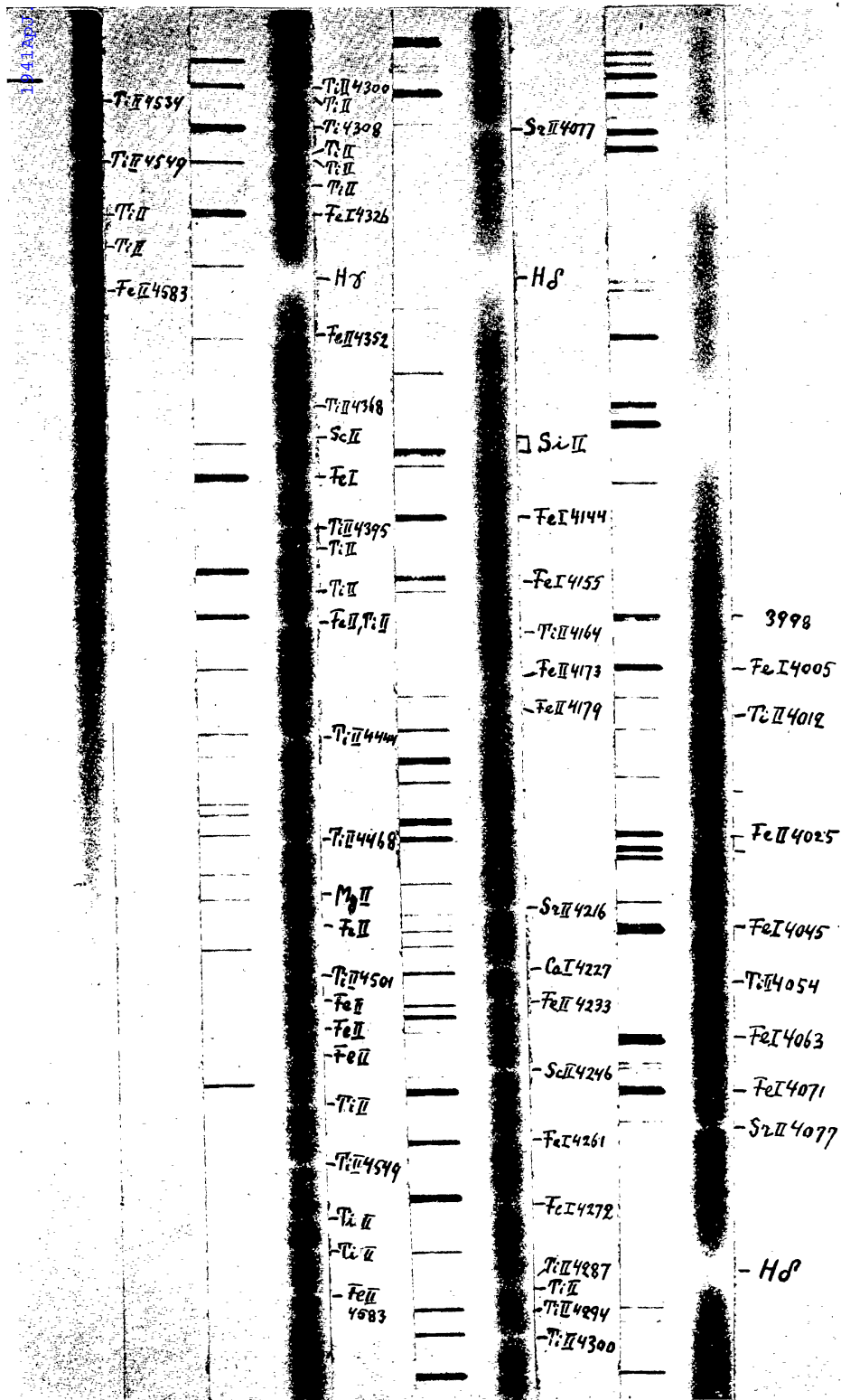
THE SPECTRUM OF 14 COMAE  
SHOWING SHARP  $H\alpha$

PLATE X



THE SPECTRA OF  $\epsilon$  AURIGAE, 14 COMAE,  
AND  $\alpha$  CYGNI

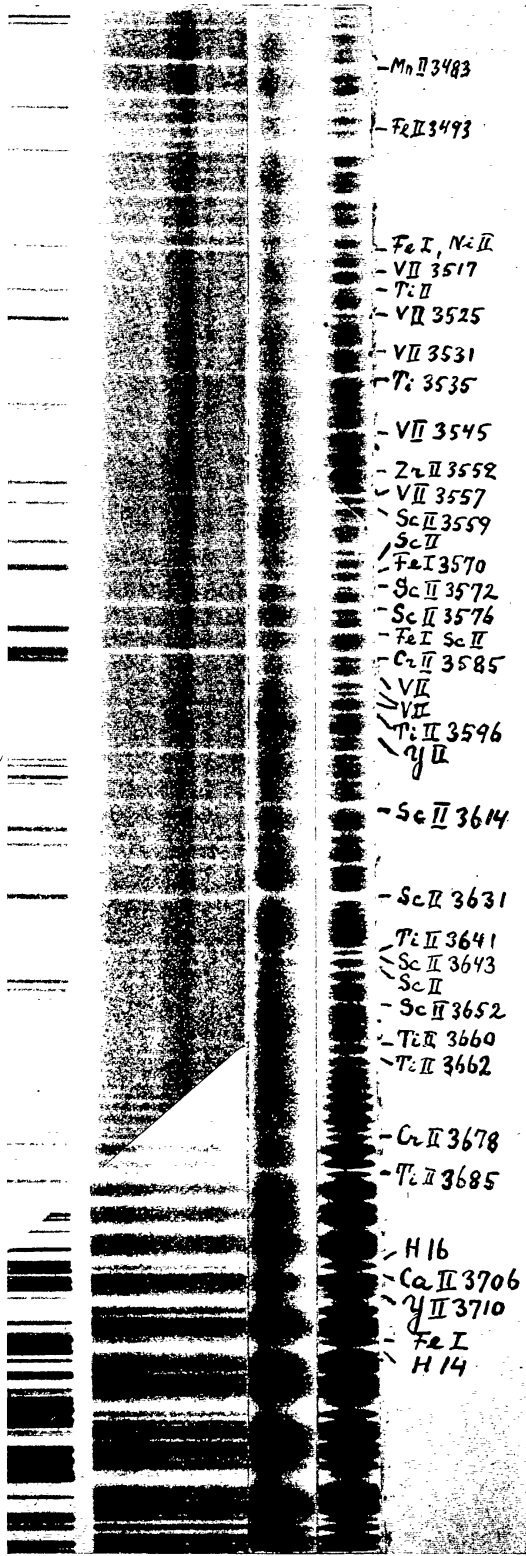
PLATE XI



THE SPECTRUM OF 14 COMAE IN THE PHOTOGRAPHIC REGION



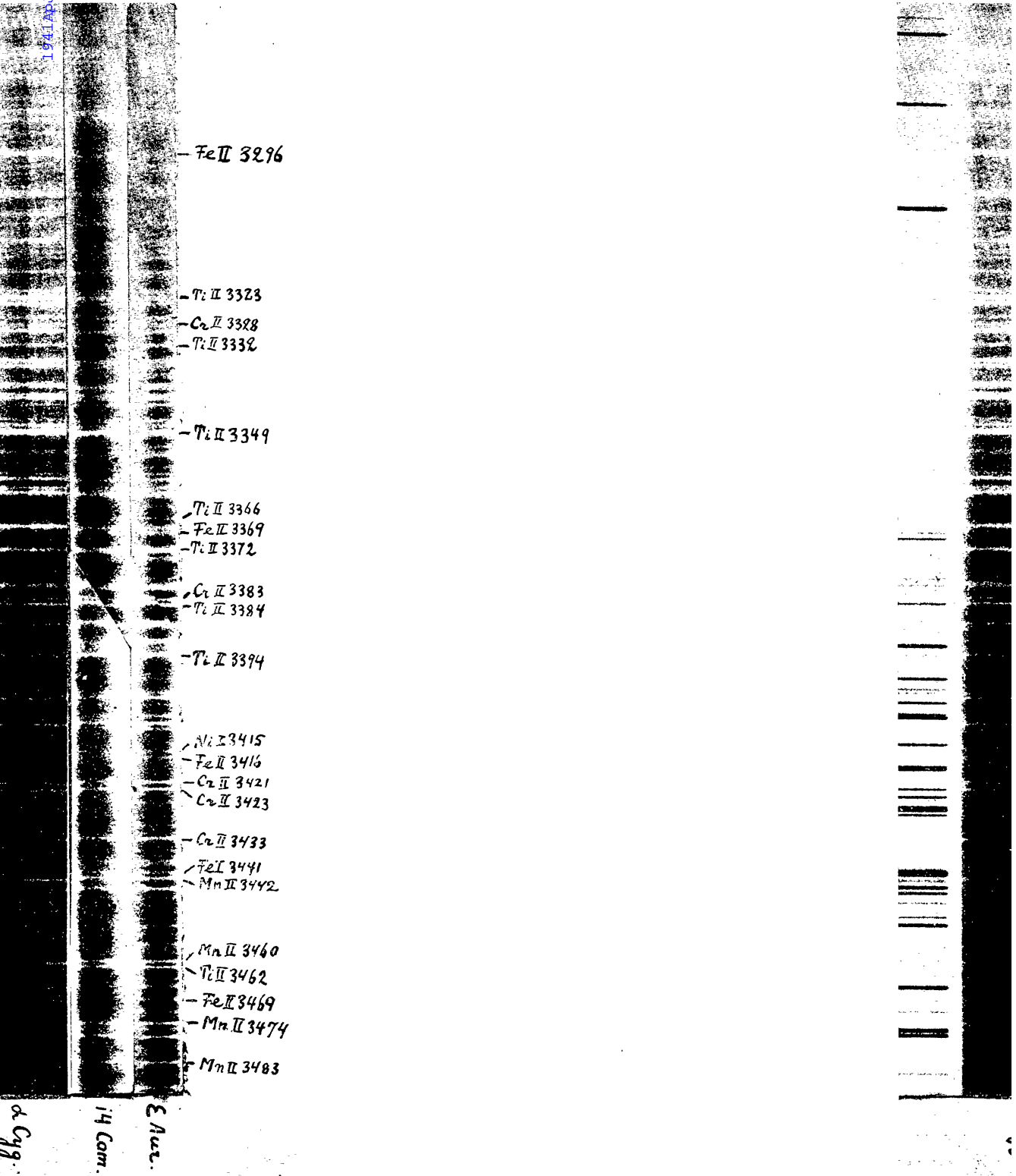
PLATE XII



THE SPECTRA OF  $\epsilon$  AURIGAE,  $\iota_4$  COMAE, AND  $\alpha$  CYGNI

194130J...291S

PLATE XIII



SPECTRA OF ε AURIGAE, 14 COMAE, AND α CYGNI

THE SPECTRA OF